UNIVERSIDADE D
COIMBRA

André Neutel dos Santos Garcia

MECHANICAL AND TRIBOLOGICAL CHARACTERIZATION OF CARBON FIBER REINFORCED POLYMER (CFRP) FOR AEROSPACE APPLICATIONS

Dissertação no âmbito do
Mestrado em Engenharia Mecânica na área de Produção e Projeto

orientada por
Doutor Luís Miguel Cardoso Vilhena Pereira da Silva
e
Professor Doutor Amílcar Lopes de Carvalho

apresentada no
Departamento de Engenharia Mecânica
Faculdade de Ciências e Tecnologia
Universidade de Coimbra

Julho de 2023

1 2 9 0

FACULDADE DE CIÊNCIAS E TECNOLOGIA
UNIVERSIDADE D COIMBRA

Mechanical and Tribological Characterization of Carbon Fiber Reinforced Polymer (CFRP) For Aerospace Applications

A dissertation submitted in partial fulfilment of the requirements for the degree of Master in Mechanical Engineering in the speciality of Manufacturing and Design

Caracterização Mecânica e Tribológica de Polímeros Reforçados com Fibra de Carbono (PRFC) Para Aplicações Espaciais

Author

André Neutel dos Santos Garcia

Advisors

Doutor Luís Miguel Cardoso Vilhena Pereira da Silva, Investigador

Doutor Amílcar Ramalho, Professor Catedrático

Jury

President	**Doutora Ana Paula Bettencourt Martins Amaro** **Associate Professor of Universidade de Coimbra**
Member	**Doutor Mário Simões Correia** **Assistant Professor of Instituto Politécnico de Leiria**
Advisor	**Doutor Luís Miguel Cardoso Vilhena Pereira da Silva** **Assistant Researcher of Universidade de Coimbra**

Coimbra, July, 2023

Agradecimentos

Os meus agradecimentos vão para todas as pessoas que colaboraram com os seus conhecimentos e o seu tempo, no sentido de eu melhor realizar este trabalho. Estou grato aos meus orientadores, Professor Doutor Amílcar Ramalho e Doutor Luís Vilhena pelo acompanhamento durante o desenvolvimento deste trabalho e pelas sugestões contínuas dadas de modo a aperfeiçoá-lo. Refiro com muita estima o empenho de Sharjeel Ahmed Khan, estudante de Doutoramento, que ao longo de toda a minha investigação, se mostrou sempre disponível e com amabilidade para me ajudar com a partilha dos seus conhecimentos. Obrigado ao Departamento de Engenharia Mecânica da Universidade de Coimbra pela disponibilização do laboratório e dos seus equipamentos cruciais na realização deste trabalho. Agradeço aos meus pais, família e amigos que sempre me apoiaram desde o início do meu percurso escolar até aos dias de hoje, acreditando sempre no meu sucesso.

Resumo

O objetivo principal do presente trabalho de pesquisa foi investigar o comportamento tribológico de um polímero reforçado com fibras de carbono (CFRP) em relação a vários metais. O estudo foi dividido em duas partes. Na primeira parte, foram realizados testes utilizando um tribómetro na configuração de cilindro cruzado para observar a interação entre um cilindro de carboneto de tungsténio e um anel feito de CFRP, titânio e um composto de ambos os materiais. Na segunda parte, o CFRP foi testado em esferas de titânio e alumínio como contra corpos.

Para ser capaz de fazer comparações, diferentes testes foram realizados com diferentes cargas aplicadas, pois isso facilitou a observação de marcas de desgaste, volume de desgaste e coeficiente de atrito. Para melhor caracterizar os resultados tribológicos, técnicas analíticas foram utilizadas, como perfilometria, microscopia óptica (OM) e microscopia eletrónica de varrimento (SEM). Com a ajuda dessas técnicas de caracterização, foi possível determinar o coeficiente de atrito, bem como a taxa de desgaste em ambas as amostras de CFRP e contra corpos correspondentes.

Como todos os testes foram realizados sem lubrificação, em condições secas, o coeficiente de atrito apresentou valores relativamente mais altos em comparação com aqueles com lubrificação.

De maneira geral, observou-se que os valores caracterizados foram influenciados pelas cargas aplicadas, pelos diferentes contra corpos utilizados nos testes, bem como pela orientação da fibra na peça de CFRP.

Palavras-chave: CFRP, Testes Tribológicos, Desgaste, Coeficiente de Atrito.

Abstract

The main goal of the present research work was to investigate the tribological behavior of a carbon fiber reinforced polymer (CFRP) against various metals. The study was divided into two parts. In the first part tests were conducted using a tribometer in cross cylinder configuration to see the interaction that we had between a cylinder of tungsten carbide and a ring made of CFRP, titanium and hybrid ring of both materials. In the second part, CFRP was tested against titanium and aluminum spheres as counter bodies.

To be able to draw some comparisons, different tests were made with different applied loads, as this made it easier to observe wear marks, wear volume, and coefficient of friction. To better characterize the tribological results, analytical techniques were employed, such as profilometry, optical microscopy (OM), and scanning electron microscopy (SEM). With the help of these characterization techniques, it was possible to determine the coefficient of friction as well as the wear rate on both CFRP specimens and respective counter bodies.

Since all the tests were performed without lubrication, under dry conditions, the coefficient of friction had relatively higher values, compared to the ones with lubrication.

In a general way, it was observed that the characterized values were influenced by the applied loads, the different counter bodies used in the tests as well as the orientation of the fiber on the CFRP piece.

Keywords: CFRP, Tribological Tests, Wear, Coefficient of Friction.

Contents

LIST OF FIGURES

LIST OF TABLES

Acronyms

Avg CoF-Average Coefficient of Friction

CFRP-Carbon Fiber Reinforced Polymer

CoF- Coefficient of friction

SEM-Scanning Electron Microscope

Std-Standard Deviation

WC- Tungsten Carbide

1. INTRODUCTION

Carbon Fiber Reinforced Polymer (CFRP) is a lightweight and highly durable composite material consisting of carbon fibers embedded in a polymer matrix. While CFRP is relatively expensive, its exceptional properties make it a preferred choice in applications where a high strength-to-weight ratio and stiffness are crucial. The aerospace industry, superstructures of ships, automotive sector, civil engineering projects, sports equipment, and a growing number of consumer and technical applications commonly employ CFRP.

In CFRP, the fibers possess greater strength than the matrix, which primarily serves to bind the fibers together. A CFRP piece comprises multiple layers of fibers that are oriented at different angles, typically alternating between 0º and 90º. The resulting structure leads to distinct regions within the CFRP piece. The top part (layer) is referred to as the unidirectional section, where all the fibers align in the same direction, providing through all the layer the same value of strength and stiffness. The cross section, known as the bidirectional part, features fibers running in two directions typically 90º apart (0º and 90º), resulting in varying strength and stiffness across the cross section (Aamir et al. 2019).

In the aerospace industry, the use of optimal materials is of utmost importance due to the sector's sensitivity and the need to minimize errors. Carbon fiber reinforced polymers and titanium find significant utilization in this domain due to their outstanding properties and advantages over other material (Hu et al. 2017; Liang and Wu 2019). CFRP, typically exhibits excellent tensile properties, good thermal and electrical conductivity, low weight and density, and high performance (Aamir et al. 2019; Birleanu et al. 2022). The microscopic structure, fiber orientation, length, and concentration contribute to the widespread use of carbon fiber composites in various industries (Birleanu et al. 2022). Titanium has been extensively employed in the aerospace industry for the past four decades due to its high strength-to-weight ratio and exceptional corrosion resistance. Recently, there has been a growing demand for titanium in non-aerospace industries due to its favorable properties (Dong 2010).

Usually, two or more layers are layered on top of one another to form a stack material, with each layer adding unique material qualities. Without the use of adhesive bonding, this

hybrid structure, which is created for particular purposes, provides performance that is noticeably better than that of a single material. In the aerospace industry stacks of CFRP and titanium are frequently used (Wang et al. 2014).

CFRP-Ti stacks are often found in primary aircraft structural components such as fuselage, wing spars, and ribs, as these structures benefit from the exceptional properties of both materials. Consequently, drilling CFRP-Ti stacks is inevitable (Khan, Emami, and Ramalho 2023). To combine these materials, they are stacked in layers, and to join them, fastener holes need to be drilled. While the properties of CFRP-TI stacks are exceptional, the machining process becomes challenging since both materials are classified as difficult-to-machine materials (Khan et al. 2023; Shyha et al. 2010). Machining these stacks presents problems such as severe tool wear, poor surface finish, and potential fiber delamination.

In this work, the drilling of the CFRP and the fretting of the CFRP against other metals was the main goal. However, it must be recreated the experiments at a laboratory scale and involve certain variations from real world scenarios. In the case of the drilling, instead of using a tungsten carbide drill against the CFRP, the CFRP material is subjected to rotational motion against a WC-Co piece that remains stationary. Similarly, in the fretting test, a metal ball undergoes cyclic motion against a CFRP piece (ball on flat configuration).

2. LITERATURE REVIEW

Over the past decades, fiber-reinforced polymers (FRP) have emerged as the predominant components in the aerospace industry due to their exceptional and distinctive properties. These materials, including carbon fiber-reinforced polymer (CFRP), glass fiber-reinforced polymer (GFRP), and aramid fibers, offer a range of advantages such as high performance, lightweight construction, increased stiffness, and superior resistance to corrosion. CFRP, specifically, finds extensive use in high-tech applications, notably within the aerospace sector. It is commonly employed in various aircraft components, including wing boxes, horizontal and vertical stabilizers, as well as wing panels. Nevertheless, CFRP has also found wide-ranging applications across diverse industries, showcasing its versatility and utility (Aamir et al. 2019).

(Liang and Wu 2019) conducted a study to explore the tribological behavior, specifically the wear mechanism of carbon fiber reinforced polymer (CFRP) in dry friction conditions against tungsten carbide. This research aimed to compare the effects of load, temperature and sliding speed on the experimental results. The study involved subjecting the materials to a wide range of load variations, between 50 N to 250 N. Similarly, the temperature was adjusted between 50 ºC and 250 ºC, while the sliding speed experienced changes from 20 m/min to 80 m/min. Conclusions show that increasing the applied load resulted in a corresponding increase in wear marks and CoF. The influence of temperature was complex. Initially, as temperature increased, wear also increased, however, beyond a certain point, the wear started to decrease. For sliding speed, the relationship with the CoF was nonlinear, but in a general way as the sliding speed increased the CoF tended to decrease.

In (Birleanu et al. 2022) study, the friction and wear characteristics of a pin on disk tribometer were examined, where both the pin and the disk were made of carbon fiber reinforced polymer (CFRP). The experimental investigations were conducted in two ways: the load varied from 6 N to 16N, and a slow sliding speed of 110 m/min was maintained. Both experiments focused on exploring the tribological behavior of the CFRP materials under lubricant boundary conditions. The findings of the study revealed that the presence of a lubricant (5100 4T 10 W-30 engine oil with TiO_2 Degussa P25 nanoparticles) resulted in

a lower coefficient of friction compared to the dry tests. Additionally, it was observed that the coefficient of friction decreased as the load increased.

(Nguyen et al. 2020) study was focused on investigating the influence of fiber orientation on tool wear during the edge-trimming process of carbon fiber reinforced polymer (CFRP). The CFRP material, with ply orientated at angles of 0 º,45 º,90 º and 135 º, was subjected to testing using a tungsten carbide end mill. To assess the progression of tool wear, a combination of scanning electron microscopy (SEM) and digital light microscopy was employed, enabling both qualitative and quantitative examination. The conclusions of the study indicate that the orientation of fibers plays a significant role in the observed tool wear. Among the different fiber orientated tests, the 0 º ply exhibited the least amount of tool wear, while the 45 º plies experienced the most significant wear. Therefore, in terms of tool wear, the order of increasing severity was observed to be 0 º>135 º>90 º>45 º.

(Wang et al. 2014) studied and compared the tool wear through drilling experiments made on a CFRP-Ti stack, as well as on the individual plates of CFRP and titanium. The observations revealed different tool wear depending on the material being drilled. Edge rounding wear when drilling CFRP, and edge chipping and flank wear for the drilling of titanium. For the CFRP-Ti stack the dominant tool wear was edge rounding from drilling the top CFRP layer, while flank wear occurred from drilling the bottom titanium layer. During the drilling of the top CFRP layer, the carbon fibers effectively removed the titanium adhesion left from drilling the bottom titanium layer, and resulted in smoothed and rounded cutting edges, leading as a result in a reduce of the occurrence of edge chipping, which increases the tool life. The CFRP-Ti stack when compared to the drilling of titanium alone achieves a tool life three times bigger. This research highlights the significant benefits of process interaction when drilling the CFRP-Ti stack, demonstrating the improved tool life and performance that can be achieved through the hybrid structure.

(Hu et al. 2017) investigated the fretting behaviors and the tribological mechanisms at the interface between Carbon fiber reinforced polymer (CFRP) composites and titanium alloy in a ball-on-flat configuration. The study evaluated the influence of fiber orientation, ambient temperature, surface treatment, and interface conditions. The tests were conducted using a stroke length of 100 μm and a frequency of 10 Hz. A load of 100 N was applied as the titanium ball rubbed against the CFRP for a duration of 20 minutes, equivalent to 12000

cycles. The experiments were performed at various temperatures (-25 ºC, 20 ºC, 75 ºC, 120 ºC, and 160 ºC) and different fiber orientations (longitudinal, 45 º, transversal, normal, 60 º, and 30 º). The results indicated that the coefficient of friction (CoF) and wear are strongly dependent on the fiber orientation and temperature. Moreover, different orientations exhibited different temperatures ranges for the highest and lowest CoF values. This means that the temperature at which the CoF was highest in the normal direction was not the same as that for the longitudinal direction. Specifically, for the normal direction, the CoF was highest at -25 ºC and lowest at 120 ºC, with the CoF decreasing as the temperature increased. In contrast, for the longitudinal direction, the CoF was highest at 160 ºC and lowest at 75 ºC. Generally, a decrease in temperature resulted in a decrease in CoF for the longitudinal direction.

(Li et al. 2018) conducted a study on the tribological behavior of carbon fiber reinforced polymer (CFRP) in fretting contacts against a titanium alloy (Ti6Al4V). The investigation employed a ball-on-flat configuration and involved the characterization of the coefficient of friction (CoF) and the wear marks. The study examined the effects of fretting amplitude, fiber orientation, load, and frequency on the tribological properties. The results revealed the increasing of the fretting amplitude led to an elevation in both the CoF and wear marks. Conversely, as the load increased, the CoF tended to decrease. The relationship with frequency was not linear, as it occasionally increased and sometimes decreased with higher frequencies. Regarding the orientation of the fibers, the CoF reached its minimum value when the fiber orientation was parallel to the sliding direction, while the maximum value occurred when the fiber orientation was perpendicular. This study demonstrated that all the factors mentioned previously influenced the CoF, with the following order of influence: fretting amplitude>applied load>fiber orientation>frequency.

(Suo et al. 2022), studied the wear damage mechanism of a bolted joint made of CFRP and titanium alloy. To investigate the influence of the fibers, tests were made using an oscillating reciprocating friction wear device with a ball on flat configuration. Four different fiber angles were used on the testing, 0 º, 30 º, 60 º and 90 º. The conclusions obtained from the study reveal that the orientation of the fibers has a significant impact on the CoF and wear behavior. As the fiber angle increased, both the CoF and wear decreased. The highest CoF and wear were observed at 0 º, while the lowest CoF and wear were found on 90 º. The

results demonstrate strong tribological anisotropy, and it is evident that the wear damage at 0 º is more severe compared to wear at 90 º.

2.1. Hertzian contact theory

For the understanding of some results presented in this work it is important to introduce the Hertzian contact theory for the crossed cylinders configuration. In the first part of this work this theory is going to be used due to the contact between WC-Co samples and the respective counter bodies (rings).

(Stachowiak and Batchelor n.d.) in their book discussed this theory and provided predictions regarding the contact area between two cylinders that are in contact. The wear mark is either a circle, elliptical or rectangle, it depends on the angle of positioning of the cylinders and the diameter of each one. If the angle of contact is parallel a rectangle contact will appear. If the diameters of the cylinders are the same and the contact is 90º we have a point, contact (circular). And for a different diameter of the cylinders with 90º contact an elliptical contact is shown.

In the present work, the contact between the WC-Co samples and the rings is considered a cross cylinder geometry, where the angle of contact was 90º, as showed on Figure 2.1 taken from (Valentin Popov n.d.). Since the diameter of both our samples were different, elliptical contact is what is expected to observe on the optical microscopy for the wear marks.

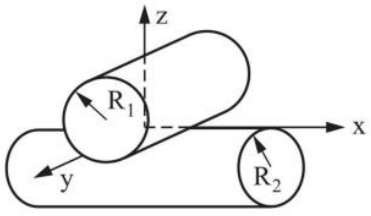

Figure 2.1. Cross cylinders contact (Valentin Popov n.d.).

3. MATERIALS, EQUIPMENTS AND EXPERIMENTAL

3.1. Materials

During the present study, various samples were utilized with different combinations, constituting different tribopairs. The sample set comprised CFRP rings, titanium rings, CFRP-Titanium hybrid rings, tungsten carbide cylinders and different spheres of titanium and aluminum.

3.1.1. Samples

Regarding the composition:

- The CFRP samples were Carbon fiber reinforced polymer plates with a thickness of 7.3 mm were procured from INEGI, fabricated at 5 bar of curing pressure in an autoclave chamber using Hexply® 8552 prepreg arranged in a (0 º,90 º) orientation. The prepreg has an amine cured epoxy matrix with unidirectional fibers having a fiber diameter of 6.6±0.3 μm. The prepreg sheets are layered one above another to obtain the finished and cured CFRP plate with a fiber volume fraction of 57% and tensile strength of 75 MPa.
- The titanium utilized in the experiments was a high-strength titanium alloy known as Ti6Al4V, distinguished for its excellent corrosion resistance and specific strength.
- The anodized aluminium 2024 was employed in the tests that had underwent T6 heat-treatment.
- The Tungsten carbide utilized had a composition of 10 % cobalt (WC-Co).

Regarding the structure:

- The rings used in the experiments were identical in size, with a diameter of 40 mm. The only distinction between them lies in the material composition as shown in Figure 3.1.

- As for the spheres, both aluminium and titanium variants had a radius of 5 mm.
- The cylinders employed possessed a diameter of 10 mm.
- The CFRP piece utilized in the tests had a thickness of 7.3 mm.

To obtain the form of a ring, abrasive water jet machining was used. The rings had an outer diameter of 40 mm and inner diameter of 30 mm from the CFRP plate to expose the fibers acting perpendicular from maximum effect during the tribological test.

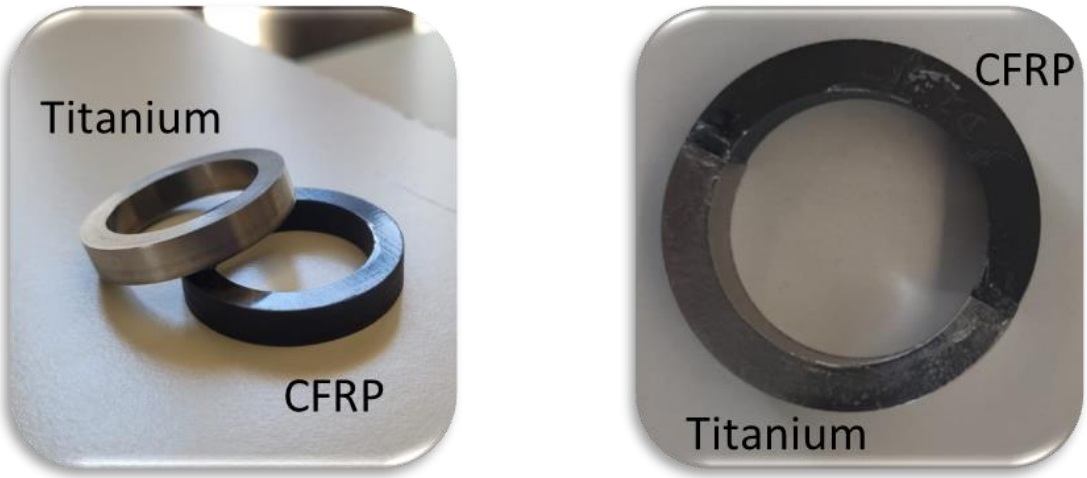

Figure 3.1. Rings used on the tests

3.1.2. Orientation of the fibers

CFRP specimen used for the test is metallography prepared by mounting the sample in acrylic resin and top part (layer) and the cross section was examined in the optical microscope. The layer part that is represented on Figure 3.2 a) and b), show the carbon fibers aligning in alternating orientations, being the first one parallel to the length of the structure (0 º degrees) and the next one perpendicular (90 º degrees). The cross section as shown in Figure 3.2 c) and d), it is possible to observe the same carbon fibers as seen above but, in this case, they are coming in two directions, bidirectional, one in 0 º and the other one at 90 º at the same time.

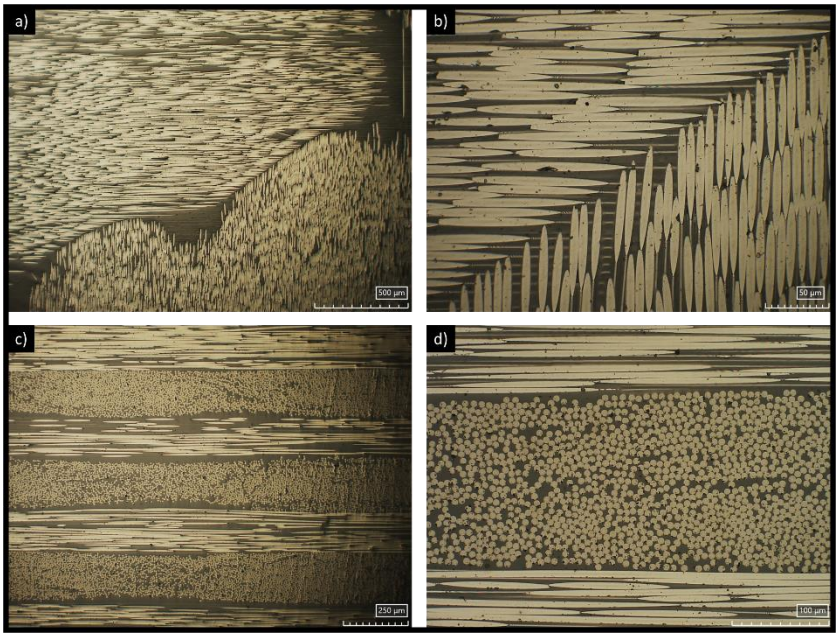

Figure 3.2. 3D digital micrographs showing the CFRP layers (a and b) and respective cross section (c and d).

3.2. Equipments

Specific equipment must be used in order to carry out the tribotesting and the consequent characterization. Each piece of equipment that was employed served the purpose of characterizing the experimental data by providing the CoF, the wear volume profile, more enlarged and more magnified photos of the sample, as well as their composition.

3.2.1. Optical Microscope

The optical microscope, also known as a 3D digital microscope, is a microscope variant that utilizes visible light and a series of lenses to produce enlarged images of small objects. In this work an HIROX HRX-01/RX-100 was utilized to see the wear marks that were on the samples in a bigger magnification.

Figure 3.3. 3D digital optical microscope Hirox.

3.2.2. Scanning Electron Microscope

A scanning electron microscope (SEM) is an essential tool utilized in scientific research, materials analysis, and various interdisciplinary fields. It provides a highly detailed and magnified view of a sample's surface, facilitating the examination of its microstructure and composition. The fundamental operating principle of a SEM involves the utilization of a high-energy electron beam, in contrast to the light used in optical microscopes. Electrons

are emitted from an electron source, typically a heated filament or a field-emission gun and propelled towards the sample using an electric field. These accelerated electrons form a focused beam that systematically scans the surface of the sample in a raster pattern. In this case the HITACHI SU-3800 model was employed, as illustrated in Figure 3.4.

Figure 3.4. Scanning electron microscope Hitachi SU-3800.

3.2.3. Tribometer

A tribometer is an instrument designed to measure various tribological parameters, including Tangential force, Normal force, and provoke or induce wear volume, between two contacting surfaces. Tribology is the science and technology that study the interaction of surfaces in relative motion and study wear, friction, and lubrication. In the specific context of this work, the tribological behaviour of the samples was investigated, necessitating the utilization of a tribometer for conducting the tests. The tribometer employed in this study was constructed and assembled at the Department of Mechanical Engineering at the University of Coimbra. The experimental setup involved two distinct configurations, as shown in Figure 3.5: initially, a static cylinder against a ring was used for contact, followed by a flat piece against a ball in the second part of the study (ball on flat configuration).

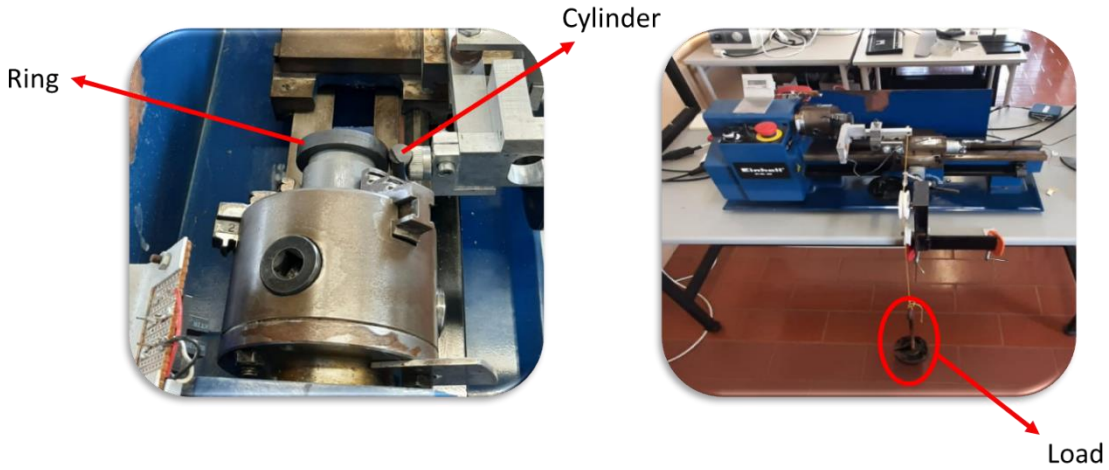

Figure 3.5. Tribometer used during experiments with: (a) cross cylinders configuration and, (b) ball on flat configuration.

3.2.4. Profilometer

A contact profilometer equipped with a delicate diamond tip was utilized to calculate the wear volume and trace profiles on the samples. Careful handling of the fragile diamond tip was essential during the process. The diamond tip with 5 μm radius, was vertically moved until it contacted the sample, and then it was moved laterally across the sample, specifically targeting the area of the wear mark, for a predetermined distance. This procedure enabled precise measurement and characterization of the wear profiles. The profilometer in use was a MITUTOYO SJ-500 (Figure 3.6).

Figure 3.6. Profilometer MITUTOYO SJ-500.

3.3. Experimental

In order to obtain a comprehensive test result, several steps were taken, as there are subsequent procedures required for the characterization of the test. The experimental process consists of multiple components, including:

1. Conducting experimental tribotests
2. Performing optical microscopy
3. Utilizing profilometry techniques
4. Employing a scanning electron microscope (SEM)
5. Carrying out complementary investigations

These steps collectively contribute to a thorough examination and tribological characterization of the test tribopair, ensuring a comprehensive understanding of the obtained results. As stated above, the experimental part consists of five distinct components. Initially, the test is initiated by ensuring proper placement and accurate values of applied load, sliding time, rotational speed (RPM), and sliding distance. This step involves taking the necessary procedures to set up the experiment correctly (Experimental tests). Once the test concludes, it becomes essential to characterize the wear mark and the coefficient of

friction (CoF). Using an optical microscope, detailed observations of the wear mark can be made, allowing the capture of photographs of both the tested body and the counter bodies (Optical microscopy). Additionally, profilometry is employed to determine the wear volume of the specific component. Multiple profiles are often taken on the same wear scar to enhance accuracy and obtain more reliable results (Profilometry). For a closer examination of the piece, a scanning electron microscope (SEM) is utilized to achieve higher magnification compared to the optical microscope used in the previous step. Finally, the gathered results are compiled, and with the aid of tools like Excel, graphs are generated, and the values for wear volume and CoF are calculated (Complementary analysis).

To ensure optimal conditions and prevent any future issues during the tests, certain preparatory procedures were conducted. Prior to commencing the tests, the samples went through a polishing process to guarantee their suitability and minimize interference with the results. The tungsten carbide cylinders were polished using two different monocrystalline diamond suspension, one containing 1μm diamond particles and the other 9 μm diamond particles. This polishing procedure continued until the cylinders achieved a well-polished and shiny appearance. Following this, the titanium rings used in the test were also polished. The polishing process for the rings involved utilizing sandpaper with grit values of 600, 1000, and 2000. The sandpaper sequence began with the lowest grit value and progressed to higher grit sizes gradually. The initial lower grit value sandpaper was responsible for the most substantial polishing, while the subsequent higher grit value was used to refine and enhance the surface finish. As the grit value decreased, the sandpaper contained larger particles, resulting in a more aggressive polishing action. Conversely, for higher grit values, the sandpaper had smaller particles, leading to a finer and more homogeneous polishing effect.

The primary objective of these tests was to assess the wear characteristics and the coefficient of friction exhibited by our samples. In order to achieve this, various tests were conducted on the samples, with certain parameters altered to observe the resulting differences.

The testing process was divided into two main parts:

- WC-Co Cylinder against Rings
- CFRP piece against spheres

3.3.1. Different rings sliding against WC-Co cylinder

In this scenario, a ring was rotated against a stationary WC-Co cylinder for a specific duration, without the use of any lubrication, which means dry tests in a cross cylinder configuration, as shown in Figure 3.7. These tests were performed using a tribometer, which was connected to a computer running LabVIEW software. The software facilitated the measurement and acquirement of the coefficient of friction (CoF). A total of nine tests were conducted, three tests using a titanium ring, four tests using a CFRP ring, and two tests involving a combination of both rings (the case shown in Figure 3.7). The purpose of these tests was to analyse the interaction between the rotating ring and the stationary WC-Co cylinder and evaluate the resulting wear and friction properties.

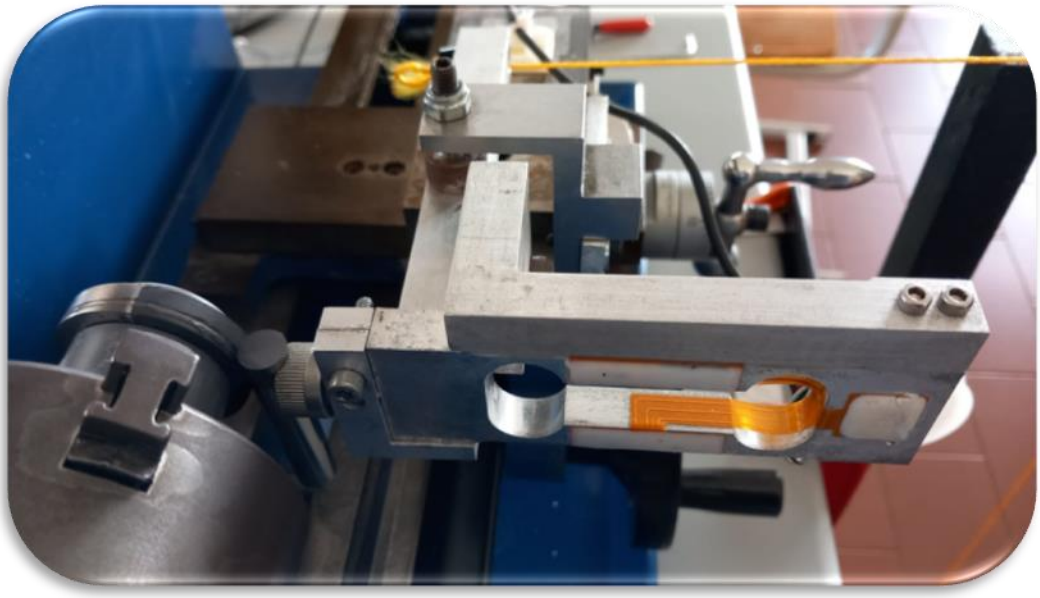

Figure 3.7. Cross cylinder configuration

3.3.1.1. Titanium ring

In the titanium ring, all three tests were conducted under very similar conditions, with the main variations being the load, sliding time, and sliding distance. The following conditions remained constant throughout the tests: the velocity was set to 120 RPM (15 m/min), and the body and counter body were unchanged. Here the only conditions that did change were the load that was 5 N, 10 N and 20 N and the sliding time that was 4000 s for

the lowest load test (5N) and for the other two it was 6000 s. Besides this two the atmospheric conditions slightly varied for each test. On Table 3.1 the values are summarized.

Table 3.1. Conditions of the tribotests for the titanium ring.

Titanium	Tribotests		
Load (N)	5	10	20
Sliding speed (m/min)	15	15	15
Rpm	120	120	120
Sliding distance (m)	1000	1500	1500
Sliding time (s)	4000	6000	6000
Temperature (ºC)	25	24	24
Relative humidity (%)	41	44	49

3.3.1.2. CFRP ring

For CFRP, the first three tests followed the same parameters as those conducted on titanium, with the only difference being the material used. Like this, the only changes were the load (5 N, 10 N and 20 N) and the sliding time (4000 s, 6000 s), as well as the atmospheric conditions. The details are summarized in the Table 3.2.

Table 3.2. Conditions of the tribotests for the CFRP ring.

CFRP	Tribotests		
Load (N)	5	10	20
Sliding speed (m/min)	15	15	15
Rpm	120	120	120
Sliding distance (m)	1000	1500	1500
Sliding time (s)	4000	6000	6000
Temperature (ºC)	25	24	25
Relative humidity (%)	34	41	47

After completing the three tests, it was possible to observe that the wear marks were significantly smaller and difficult to distinguish from one another, regardless of the load or sliding time, unlike the results obtained with titanium where the differences were noticeable.

In light of this, I conducted a new test with some modifications. In this test the sliding speed was 120 RPM, the load 20N and the biggest change was the sliding time that was 80000 s. Table 3.3 shows the summarized results.

Table 3.3. Conditions of the new tribotest for the CFRP ring.

CFRP	Tribotest
Load (N)	20
Sliding speed (m/min)	15
Rpm	120
Sliding distance (m)	20000
Sliding time (s)	80000
Temperature (ºC)	25
Relative humidity (%)	37

3.3.1.3. CFRP-Ti Hybrid ring

The two tests conducted on the hybrid ring were approached differently in order to better understand the material's transition between different materials, its wear characteristics, and the coefficient of friction (CoF). Both tests were performed at a velocity of 60 RPM and a load of 20 N. The main distinction between the tests was the time allocation.

In the first, a total duration of 5000 s was divided into six parts. The initial part lasted 100 seconds and involved the assistance of a picoscope connected to a computer for analyzing the peaks. The subsequent parts were of equal duration, each lasting 900, 1000, 1000, 1000 and 1000 s respectively, following a standard procedure similar to the previous tests. The reason for conducting five tests of 1000 seconds each was to divide the data points evenly, making it easier to process the values in Excel.

In the second test, there was no initial 100-second segment, and the total test duration increased to 6000 s, divided into the same six parts as before, with each part lasting 1000 s. For both of the tests the atmospheric conditions were 24 ºC and 34 % relative humidity. These conditions are summarized in Table 3.4.

Table 3.4. Conditions of the tribotests for the hybrid ring.

CFRP/Titanium	Tests	
Load (N)	20	20
Sliding speed (m/min)	7.5	7.5
Rpm	60	60
Sliding distance (m)	625	750
Sliding time (s)	5000	6000
Temperature (ºC)	24	24
Relative humidity (%)	34	34

Table 3.5 helps on a better explanation of the time, being the red time the one to calculate the peak and the purple the normal one.

Table 3.5. Time span for the composite tests.

	Tests	
Time(s)	5000	6000
Separated time(s)	100+900+1000+1000+1000+1000	1000+1000+1000+1000+1000+1000

3.3.2. CFRP specimen against Ti and Al spheres

In this experiment, dry tests were conducted using a tribometer to study the sliding behavior between CFRP specimens against titanium and aluminum ball with different fiber orientation to evaluate the effect of fiber orientation on the tribological properties (ball on flat configuration). Lubrication was intentionally excluded to simulate real-world dry conditions. The tribometer was connected to LabVIEW software on a computer to facilitate data acquisition and analysis. During the tests, the ball was passed through a cyclic motion with a displacement of 4 mm, and a stoke length of 2 mm. The tests were performed on both the layer and cross section sides of the CFRP specimen. A total of 10 tests were conducted using the titanium ball, while 6 tests were performed using the aluminium ball. The primary objective of these tests was to examine the wear patterns and the CoF exhibited at the contact interface between the ball and the CFRP piece.

3.3.2.1. Titanium spheres

The titanium spheres went through ten tests that were divided into two parts: five tests focused on the layer, while the remaining five tests examined the cross section. The purpose was to determine whether the orientation of the fibers played a role in wear and in the CoF. Throughout all ten tests, consistent values were maintained for the number of cycles, sliding time, frequency, sliding speed, and sliding distance. The only variables were the applied load and the specific part of the piece where the test took place.

Constant values:

- Number of cycles:110000
- Sliding time:20000 s
- Frequency: 5.5 Hz
- Rotational velocity: 330 RPM
- Sliding distance:440 m

3.3.2.1.1. Layer part

In the first five tests conducted on the top layer, a ball was used to wear down a unidirectional layer of fibers. As (Aamir et al. 2019) stated, it is expected that there will be a linear relationship between the wear and the applied load. Here the only thing that changed was the applied load, and the atmospheric conditions at the moment. The load suffers a variation of 20 N total, starting at the 10 N until 30 N with a 5 N interval. To better understand the conditions of experiment on the Table 3.6 the conditions are organized.

Table 3.6. Conditions of the tests occurred on the CFRP layer part against the titanium ball

Layer	Tests				
Load (N)	10	15	20	25	30
Temperature (ºC)	24	29	24	24	24
Relative humidity (%)	51	29	52	50	46

3.3.2.1.2. Cross section

In the remaining five tests conducted on the cross section, the ball was used to wear a bidirectional part where the fibers run in two directions, 90 degrees apart (0 º, 90 º). As mentioned in (Aamir et al. 2019), the results are expected to be varied, and it is not anticipated that there will be a linear relationship between the load and the wear in this case. Here the tests conditions were the same as the ones made to the layer part, because the main objective was to see the influence of the orientation of the fibers. Like that the tests suffer a variation from 10 N to 30 N in an interval of 5 N each test. Like previously the atmospheric conditions were different for each case. On the Table 3.7 the conditions are summarized.

Table 3.7. Conditions of the tests occurred on the CFRP cross section against the titanium ball

Cross section	Tests				
Load (N)	10	15	20	25	30
Temperature(ºC)	29	29	29	29	29
Humidity(%)	43	37	33	31	35

3.3.2.2. Aluminium balls

As predicted, and in contrast to the titanium ball, the aluminium ball underwent a higher level of wear during the experiments. Consequently, only three tests were conducted on each part of the CFRP piece using lower loads (10N, 15N, 20N) for a total of six tests. Similar to the titanium ball tests, the experiments with the aluminium ball maintained consistent values of cycles, time, frequency, velocity, and distance. These parameters remained unchanged, indicating that the experimental conditions were kept constant for both materials in order to have a fair comparison between the two materials. The only variables that differed were the applied load and the specific part of the piece where each test was conducted, the same way that happened to the titanium.

3.3.2.2.1. Layer part

As previously mentioned, this particular part will undergo only three tests. According to (Aamir et al. 2019), the strength of this part remains constant across all the layer. Consequently, we can anticipate a linear relationship between wear and load, indicating that as the load increases, the wear is expected to increase proportionally. The conditions of these tests were the same as the ones used in the titanium balls, because in this case the theme of study was the influence of the material. For that three tests for three different loads were made from the 10 N to the 20N in an interval of 5N. Once more the atmospheric conditions were different for each case. Table 3.8 better explain the conditions.

Table 3.8. Conditions of the tests occurred on the CFRP layer part against the aluminium ball

Layer	Tests		
Load(N)	10	15	20
Temperature(ºC)	28	29	29
Humidity(%)	55	55	61

3.3.2.2.2. Cross section

In the three latest tests conducted on the cross section of the aluminium ball, the ball underwent sliding against a bidirectional layer. According to (Aamir et al. 2019), the results were expected to exhibit variation and lack any discernible relationship due to the presence of two directional fibers. Like all the previous tests the main goal was to see the influence of the material and the fibers, so everything remains the same. The only thing that changed besides that, was the load that was in each test different, being 10N on the first one, 15N on the second one and 20N on the last one. The atmospheric conditions were different in each one of the tests. The conditions are presented on Table 3.9.

Table 3.9. Conditions of the tests occurred on the CFRP cross section against the aluminium ball

Cross section	Tests		
Load(N)	10	15	20
Temperature(ºC)	29	29	29
Humidity(%)	54	51	60

4. RESULTS AND DISCUSSION

This section discusses about the results obtained from different tribotest and tribological material contact as explained in the previous section. The obtained data was organized and presented through graphs, tables, and photos and was analysed to obtain variation in CoF, along with detail investigation of wear tracks in a comparative manner to establish meaningful conclusion about the tribological behavior of different material pair and will be discussed below.

4.1. Rings (titanium, CFRP and hybrid) against WC-Co Cylinder

The obtained results include graphs presenting the coefficient of friction for all the conducted tests, graphs illustrating the wear volume for each of the rings, SEM images, and additional graphs created in Excel to facilitate analysis and comparison of the results.

4.1.1. Coefficient of friction (CoF)

As mentioned earlier, the coefficient of friction (CoF) was obtained through the use of a LabVIEW program. This program recorded the CoF values during the test. Once the test was completed, the recorded values from the computer were extracted and transferred to an Excel sheet. Subsequently, graphs were created and the relationship between sliding time and CoF were displayed. Before conducting the tests and analyzing the data, it was anticipated that the CoF would be higher on the titanium material than on the CFRP material. This expectation came from the fact that titanium involves a metallic contact, whereas CFRP does not. In the case of the hybrid ring material, it was predicted that the CoF would exhibit fluctuations or variations due to the transition between different surfaces. These variations in the CoF were expected due to the composite material's composition and structure.

4.1.1.1. Titanium ring

Figure 4.1 shows the relationship between the Coefficient of friction and the sliding time for three different loads (5 N, 10 N and 20 N) for WC-Co cylinder sliding against titanium ring. The graph shows that all three tests exhibit a similar pattern. The CoF increases rapidly on start followed by a gradual decrease during the running in phase. This gradual decrease in the beginning of the test could be clearly seen in the inset graph. Subsequently, the CoF increases steadily with the increase in sliding time. However, this increase is minimal, as the values consistently surround the same CoF values. In all the tests, the steady state CoF varies from 0.5 to 0.6, with the 10 N test showing the highest CoF (0.6) and the 20 N test showing the lowest CoF (0.5). Typically, one would expect the CoF to be higher with a heavier load, but in this particular case, the 20 N test does not adhere to that expectation. Upon observation it is evident that the CoF values exhibit a slight amount of noise when compared to the CFRP rings as discussed later. This noise could be attributed to the highly adhesive nature of titanium material transferred to the WC-Co cylinder, which, at a certain point, experienced what is called a stick and slip phenomena. Stick-slip phenomena is a well-documented occurrence that frequently happens when two solid bodies slide against each other at low velocities (below 180 mm/min). Stick-slip phenomena can be observed in various contexts and have both positive and negative implications. However, in numerous engineering and technological applications, this phenomenon is undesired due to its jerky motion characterized by intermittent sticking and slipping. The consequences of stick-slip motion include vibration and noise generation, energy dissipation, increased wear on smooth surfaces, and potential damage to moving components (Birleanu et al. 2022). Consequently, each time the ring passed over those areas, it resulted in a slightly noisy variation in CoF.

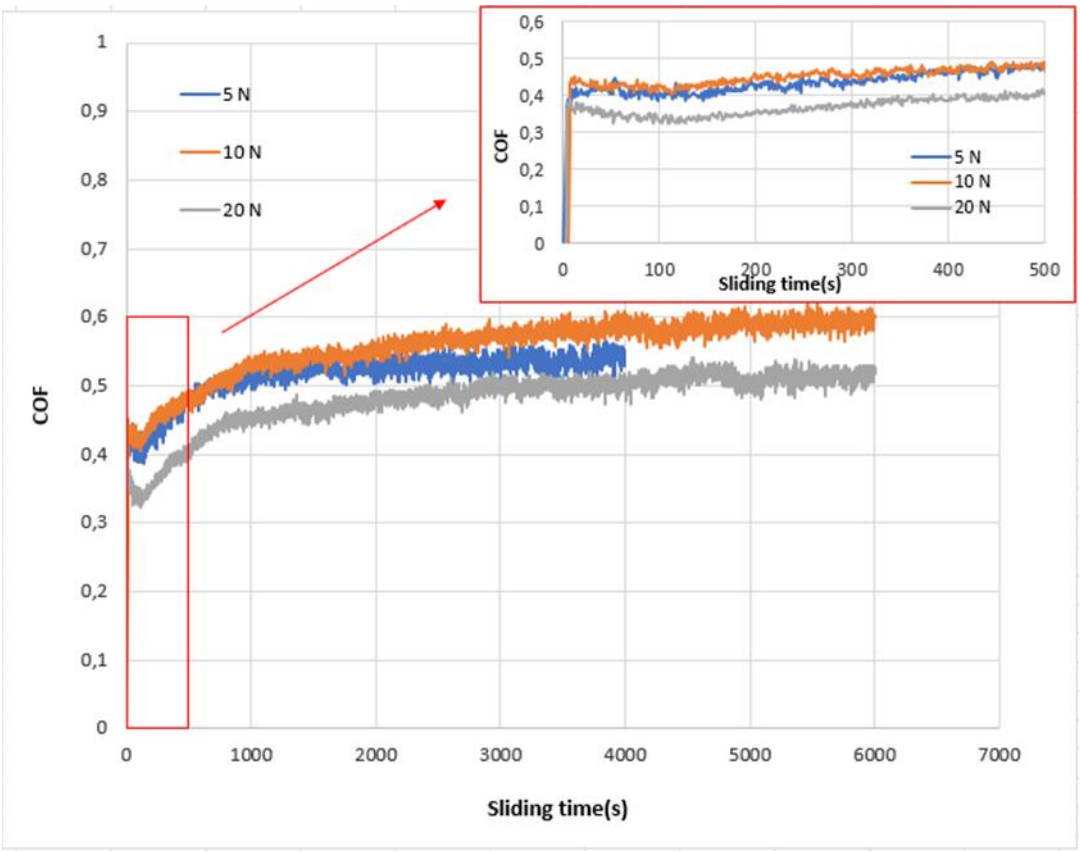

Figure 4.1. CoF vs. sliding time for the titanium rings sliding against WC-Co cylinder for three different loads (5, 10 and 20 N).

4.1.1.2. CFRP ring

Figure 4.2 illustrates the correlation between the Coefficient of friction and the sliding time for three different loads (5 N, 10 N and 20 N) for CFRP ring sliding against WC-Co cylinder. The graph shows that the running-in occurs very fast in the first 10-15 sec and steady state of CoF was reached and remained consistent with the increase in sliding time. In the inset graph, it is possible to clearly observe that the running was indeed very small. Throughout the entire duration of the tests, the CoF values remain relatively stable with minimal to no fluctuations, and variation in CoF ranges from 0.2 to 0.25. The test conducted with a load of 5 N demonstrates the lowest CoF (0.19), while the test with a load of 20 N exhibits the highest CoF (0.25). Unlike the test against titanium ring, the CoF for this particular material (CFRP) does not display any fluctuation or noise. The CoF remains constant throughout the test, indicating the absence of stick and slip phenomena to CFRP and the consistent nature of the frictional properties.

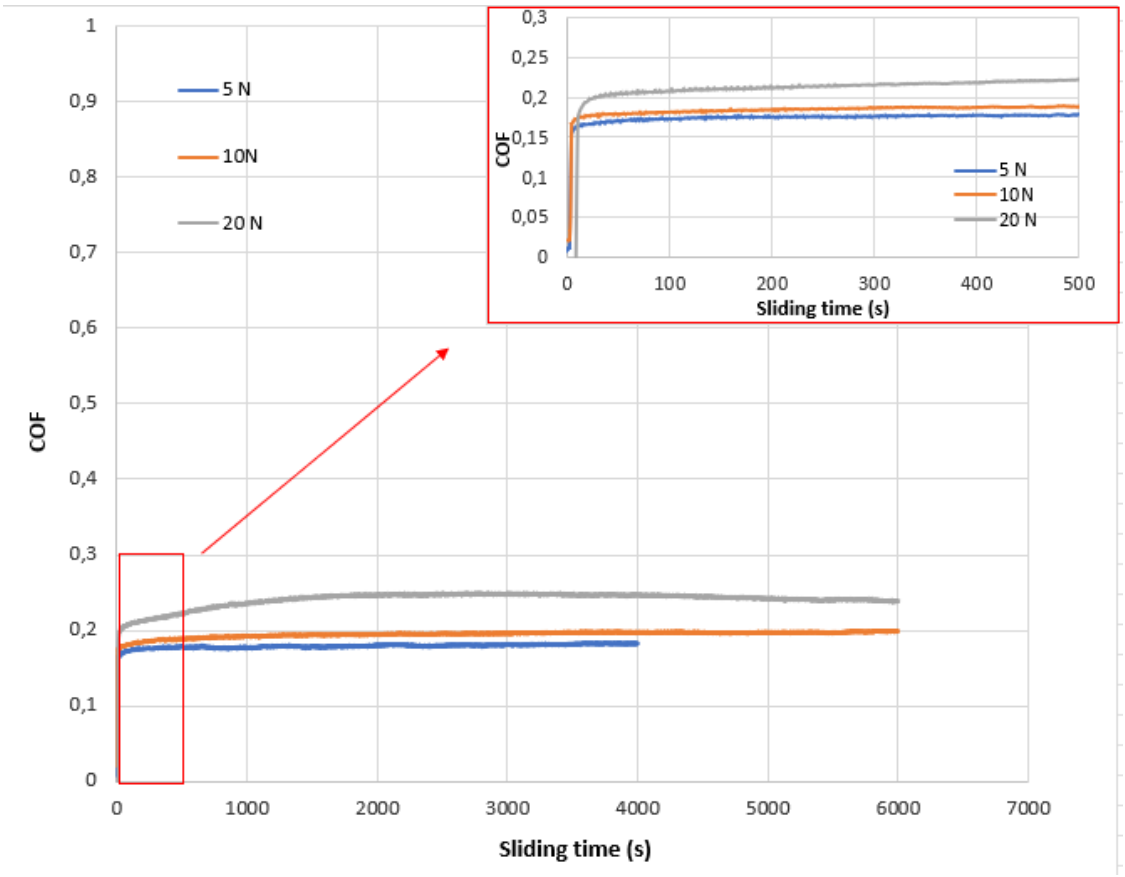

Figure 4.2. CoF vs. sliding time for the CFRP rings sliding against WC-Co cylinder for three different loads (5, 10 and 20 N).

4.1.1.3. Hybrid ring

For the hybrid ring of CFRP and titanium, two different tests were made for total sliding time of 5000 s and 6000 s, but the results were very similar. Therefore, the result of the test with the longest sliding time (6000 s) will be discussed. For the hybrid ring the Coefficient of friction has a very different behavior because the WC cylinder is contacting going against two different materials i.e. CFRP and titanium from time to time as described previously, which means that the CoF is going to have variations every time the material is changed. Figure 4.3 (a) show CoF variation with sliding time for Hybrid ring sliding against WC-Co cylinder. In the beginning of the test, the CoF shows high fluctuation ranging from almost 0.2 to almost 0.6 while near the end of the test the values are ranging from 0.2 to 0.3. In the mini graphs presented below, three different sets of time were highlighted, that is in the beginning (b), in the middle (c) and in the end of the test (d). These graphs show clear variation in fluctuations on the CoF with the increase in sliding time. Figure 4.3 (b) indicate the beginning of test showing clearly distinguishable cyclic variation when sliding against titanium and CFRP part, and a rapid transition when passing from one to the other. But as time passes by, as shown in Figure 4.3 (c) and (d) we can observe significantly reduced fluctuations and amplitude in CoF variation and considerably smooth transition between the different materials of the hybrid ring. This might be due to the transfer of each material onto one another and active mixing and shearing favoring material transfer from tribological interaction. For example, the wear of the CFRP ring due to time move to titanium and some material tends to stay on the titanium part and the same goes to the titanium on the CFRP part. In order to elaborate further, the WC cylinder with the increasing time in the test would be sliding against composite contact which was formed by the transfer of material forming a complex mixture different from the actual material. Therefore, the variation in CoF amplitude was reduced altogether near the end of the test.

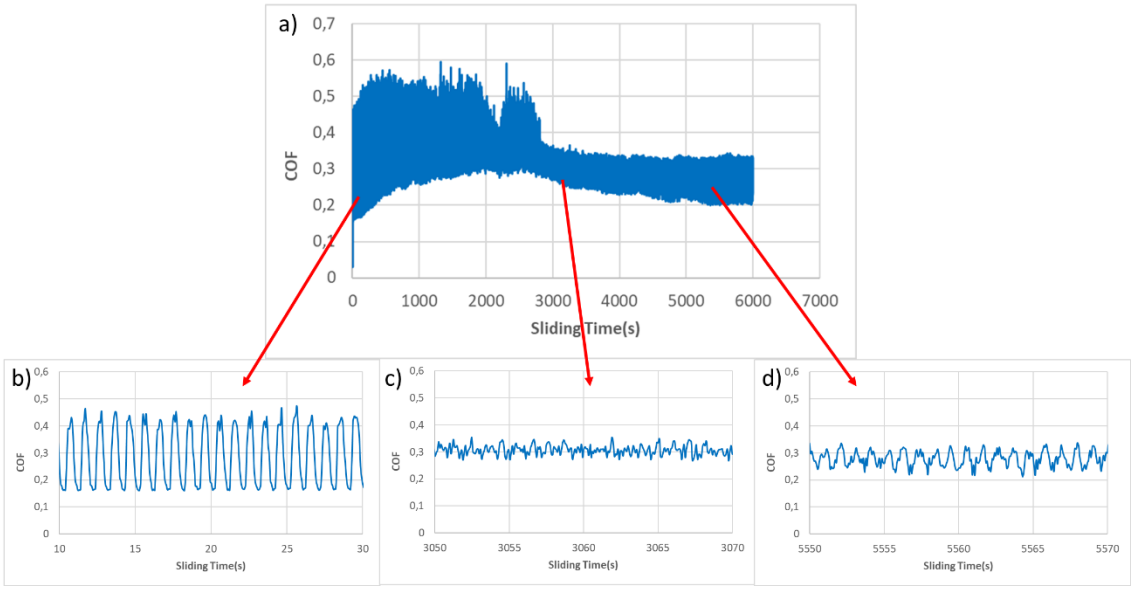

Figure 4.3. CoF variation for the hybrid rings sliding against the WC-Co cylinder.

In order to confirm the formation of composite contact and active transfer of the material between the WC and hybrid ring and its constituents, SEM and EDX analysis was performed. The sample used for analysis was a cross-sectioned piece of the titanium from hybrid ring which was mounted and polished prior to examination. Figure 4.4 show that severe damage was caused from the tribological contact of WC sliding, resulting in micro-fracture to the titanium. The EDX analysis clearly show that the contact was completely transformed after the test, which could be confirmed from the presence of large amount of carbon element beneath the titanium. It is possible to understand that the carbon existence on the contact region was from the wear of the CFRP which was transferred to the titanium part of the ring. As the tests prograte the CFRP and the titanium started to get transferred on all the contact region of the ring and not only in their own part, making the CoF more homogenic and less noisy on the transition. Therefore, in the beginning as exchange of material was lower, the CoF showed large amplitude variation and with visible transitions from one material to another but with time it leads to a more consistent CoF and relatively smooth transition, because the active contact was completely transformed.

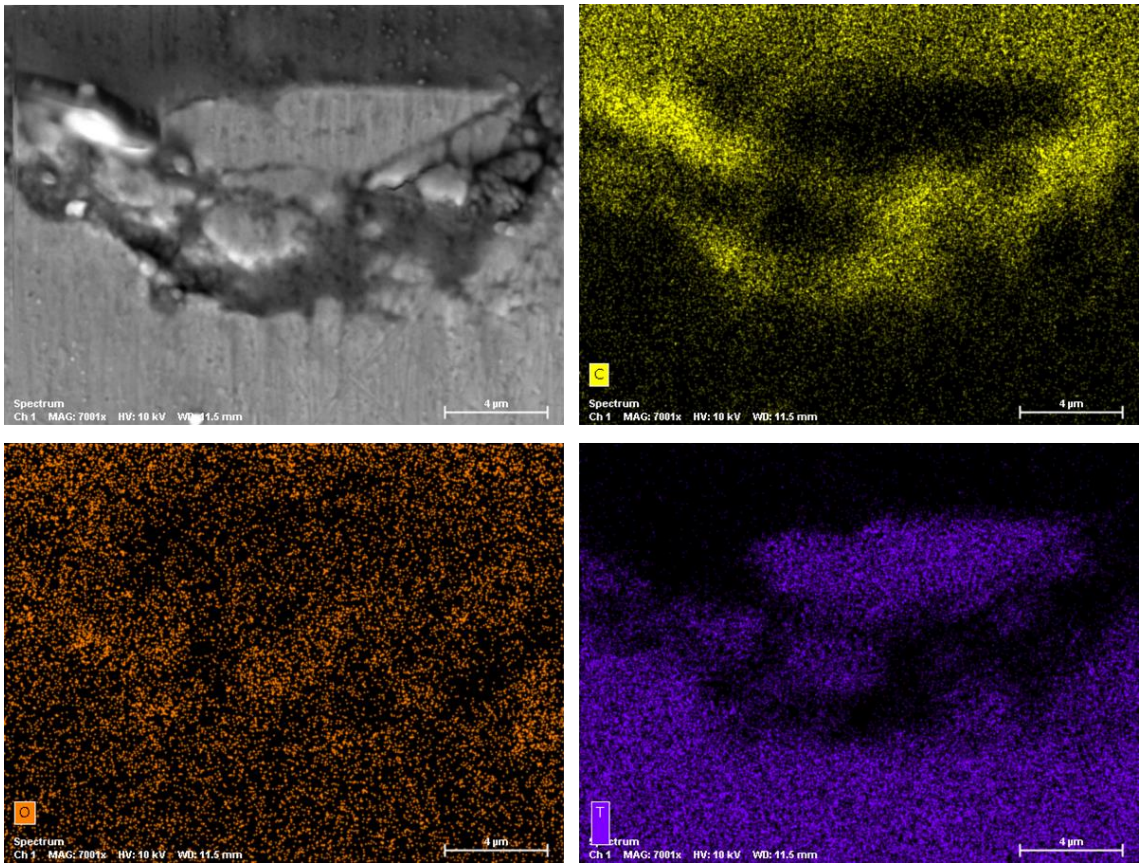

Figure 4.4. SEM/EDS mapping, showing micrographs of the titanium part of the hybrid ring.

4.1.2. Wear volume

4.1.2.1. Titanium ring

Figure 4.5 demonstrates a tendency between the depth and the length of the wear track and the corresponding applied loads (5 N,10 N and 20 N), providing clear insights into the wear characteristics. As anticipated, the wear volume consistently escalated in correlation with the increase in applied load. Every time the load was increased, the wear volume increased. Notably, the lowest volume wear was observed at 5 N (lowest load) with a value of 4.20E-07 mm^3, while the highest wear volume occurred at 20N (highest load) with a value of 1.58E-05 mm^3.

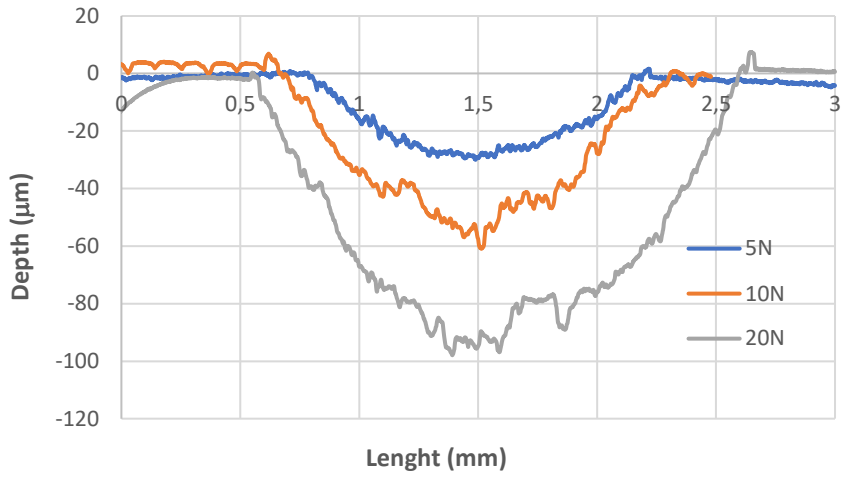

Figure 4.5. 2D profiles on wear track of the titanium rings, sliding against a WC-Co cylinder under different applied loads (5, 10 and 20 N).

4.1.2.2. CFRP ring

Since the wear on the CFRP ring was very low for the first three tests (the same ones made to the titanium) it was not possible to measure and quantify the wear volume. That's why a fourth test was made, just for the CFRP to see if some wear volume was able to be calculated. The Figure 4.6 represents that test that had a duration of 80000 s with an applied load of 20 N.

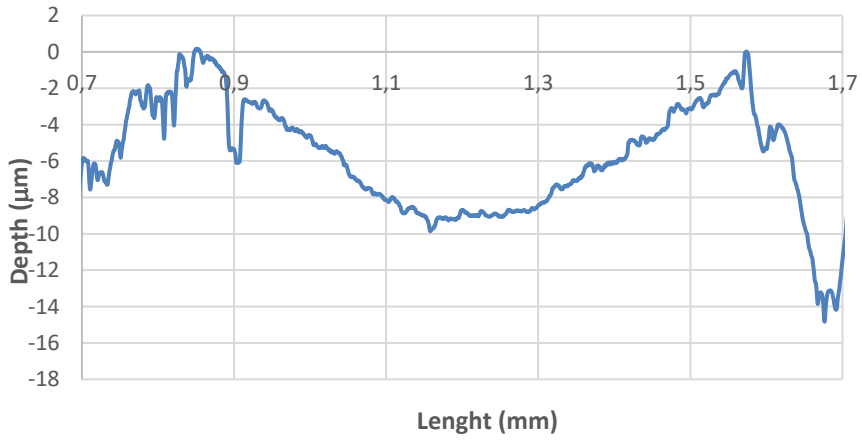

Figure 4.6. 2D profile from the cross-section wear track of the CFRP ring, sliding against a WC-Co cylinder under 20 N applied load.

Figure 4.6 demonstrates that under severe conditions the depth and length of the wear track increases. Here the wear volume got a value of 2.62E-07 mm^3, which means that in comparison to the titanium ring this value, for an applied load of 20 N and for a sliding time of 80000 s, is lower than the test with lowest wear volume, that was for test with 5 N applied load and 4000 s sliding time. It shows that the wear on the CFRP ring is much lower than the one that happened to the titanium, independent of the conditions.

4.1.2.3. Hybrid ring

In terms of wear volume, when analyzing the hybrid ring, separate graphs for the titanium component, Figure 4.7, and for the CFRP component, Figure 4.8, were generated. In both graphs there is a relation between the depth and the length for two different tests (5000 s and 6000 s). It was evident that as time progressed, there was a noticeable increase in wear volume for both materials. However, when comparing the effects of a 1000 s increment, like on the second test, it became apparent that the titanium component exhibited a significantly greater rise in wear volume compared to the CFRP component. Since the wear volume of the CFRP increased from 1.30E-06 mm^3 to 1.49E-06 mm^3 while the wear volume of titanium had on increase from 1.00E-06 mm^3 to 1.74E-06 mm^3.

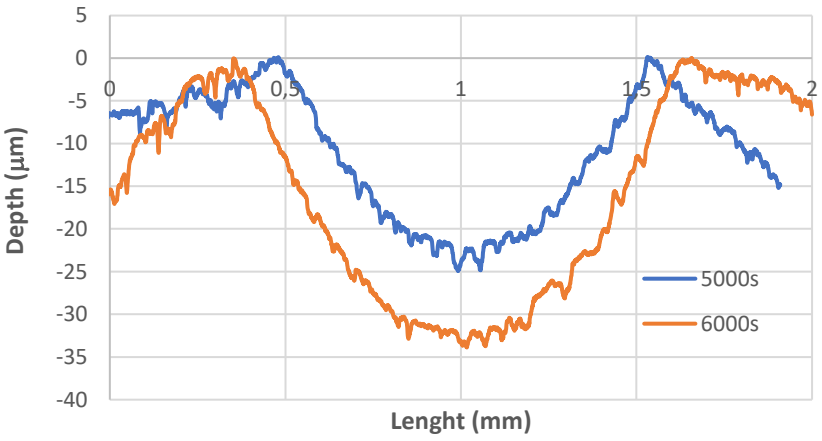

Figure 4.7. 2D profiles from the cross-section wear tracks of the hybrid ring (titanium part), sliding against a WC-Co cylinder under different sliding times (5000 and 6000 s).

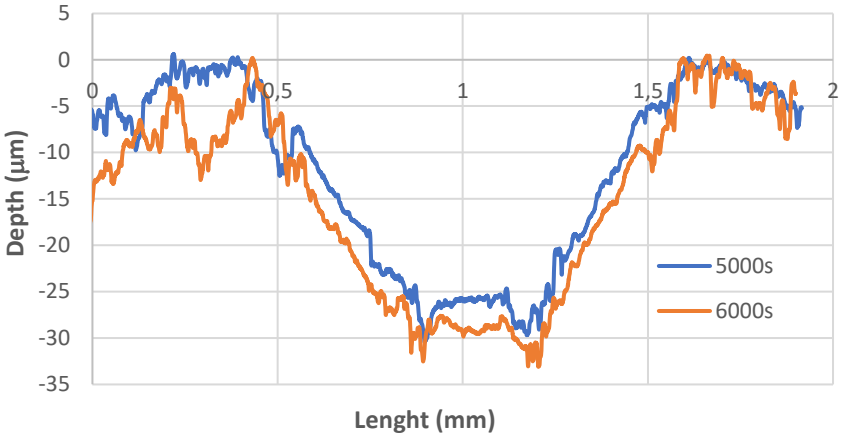

Figure 4.8. 2D profiles from the cross-section wear tracks of the hybrid ring (CFRP part), sliding against a WC-Co cylinder under different sliding times (5000 and 6000 s).

4.2. CFRP specimens sliding against Ti and Al spheres

The section will present optical microscopy of the wear region of CFRP specimen and both titanium and aluminium spheres used as counter bodies, as well as graphs displaying the CoF for all the conducted tests. Additionally, there are graphs illustrating the wear volume for different parts of the CFRP specimen (layer and cross section) and SEM images.

4.2.1. Coefficient of friction

4.2.1.1. Titanium sphere

4.2.1.1.1. Layer part

Upon analysing the Figure 4.9, that show the CoF with the number of cycles, for different applied loads, it is evident that there are similarities across all the tests. Firstly, it is notable that all of them exhibit a significantly high CoF at the beginning, around 0.4, in comparison to the subsequent portions of the test, around 0.25. This can be attributed to the initial running in process, which is more pronounced in the mini graph. The CoF value initially increases but then stabilizes around the same level at approximately 600 cycles, which remains consistent throughout all the tests. Following the running in process, the CoF values across the tests vary between 0.2 and 0.25. This indicates that there are numerous

similar values within a narrow range of 0.05, even though there is a 20 N difference in the applied loads. The highest CoF value observed is 0.25, corresponding to the 10 N test (which represents the lower force value). Conversely, the lowest CoF value is observed in the 25 N test, as it experiences the most significant decrease in the CoF value from the beginning until the end of the test.

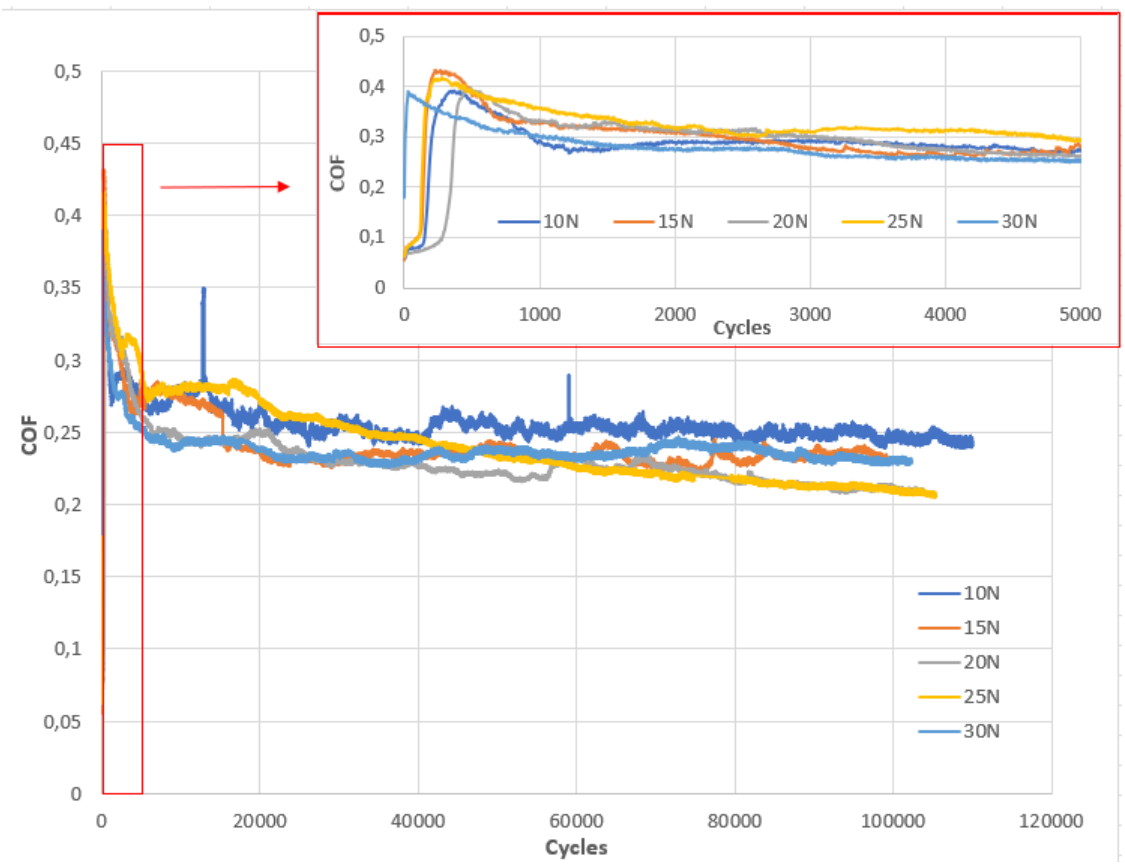

Figure 4.9. Evolution of the CoF with the number of cycles for the CFRP specimen sliding against a titanium sphere (layer part).

To compare the CoF values with the different applied loads, the average CoF and standard deviation were calculated. In this case, the calculations were performed for 15000 cycles, i.e. from 75000 to 90000 cycle. Based on these calculations the Figure 4.10 shows the graph created to better see and compare the results.

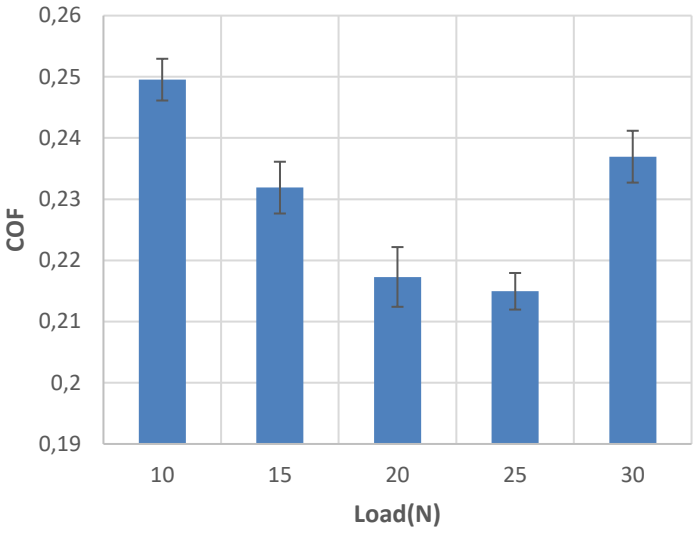

Figure 4.10. Steady state CoF for different applied Loads for the CFRP specimen (layer part) sliding against titanium spheres.

On the graph, load is against the CoF while representing the standard deviation as error bars. As seen on Figure 4.910, it is evident that the 25 N test exhibits the lowest CoF, with approximately 0.215 while the 10 N test displays the highest CoF of 0.25.

4.2.1.1.2. Cross section part

Figure 4.11, show the evolution of the CoF with the number of cycles, for different applied loads on cross-section CFRP. The same to what happened on the layer part, where all of them exhibit a significantly high COF at the beginning, around 0.33, in comparison to the subsequent portions of the test, around 0.25 or 0.15. This initial increase in CoF can be attributed to the running in progression, that for better understandable is pronounced in the mini graph. After approximately 1000 cycles, the CoF value remains relatively constant without any significant decrease or increase. Following the running in process, the CoF values in the tests vary between two specific values. The first three tests (10 N,15 N and 20 N) all have a very similar CoF value, rounding to approximately 0.15. On the other hand, the last two tests with higher loads (25 N and 30N) exhibit a CoF value of 0.24. Among these, the test with the highest CoF is the 25 N applied load, while the 20 N or 15 N applied loads have the lowest CoF.

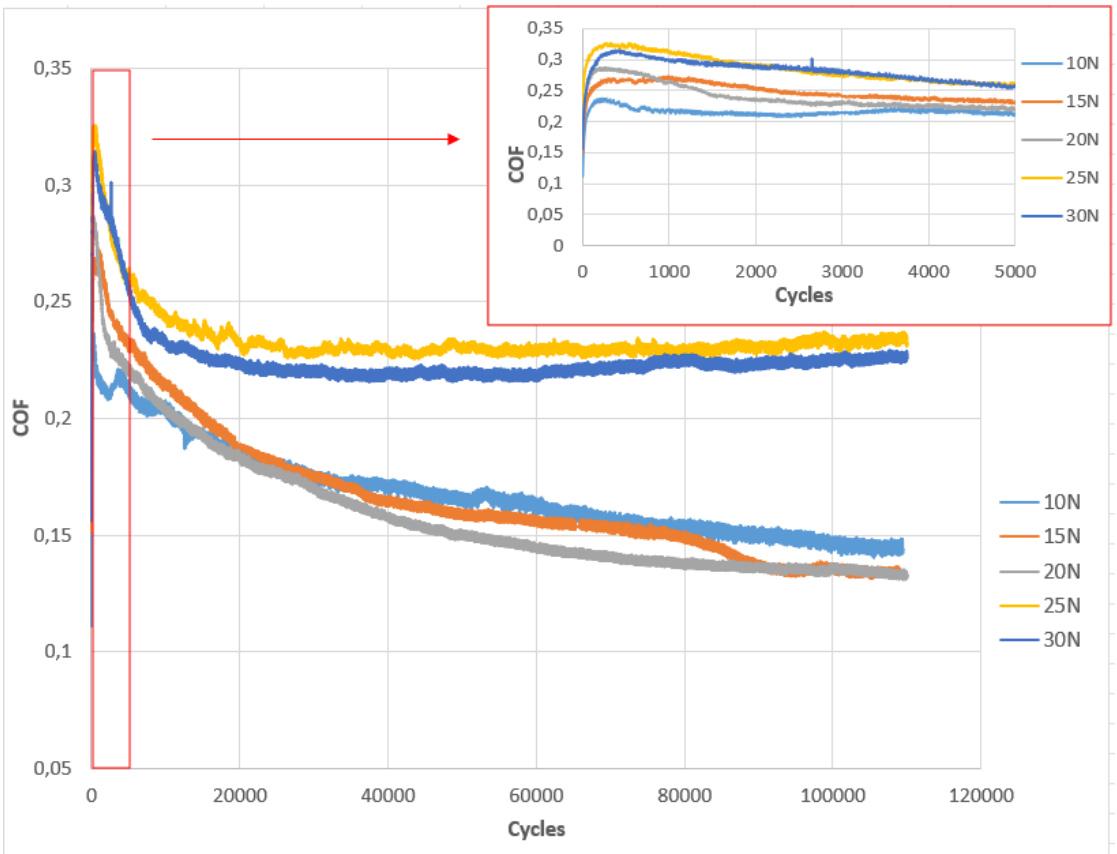

Figure 4.11. Evolution of the CoF with the number of cycles for the CFRP specimen sliding against a titanium sphere (cross section part).

The CoF values were compared with the load, and calculations were made to determine the average CoF and standard deviation for the same number of cycles (15000 cycles from the 7500 to the 9000). Based on these calculations, Figure 4.12, was generated.

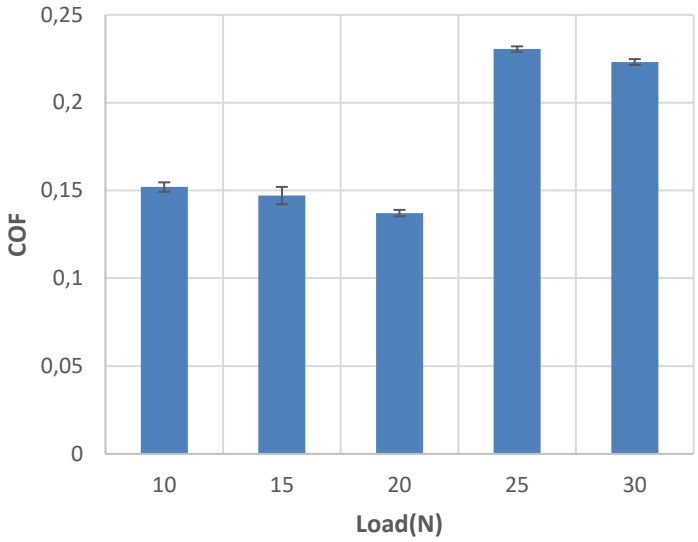

Figure 4.12. Steady state CoF for different applied Loads for the CFRP specimen (cross section part) sliding against titanium spheres.

The graph shows the load against the CoF, and the standard deviation represented as error bars. Like seen previous on Figure 4.12, we can observe the presence of two different CoF values: approximately 0.15 for the first three loads and around 0.23 for the last two loads. Additionally, it can be observed that the lowest CoF value is associated with a load of 20 N (0.137), while the highest CoF value corresponds to a load of 25 N (0.23).

4.2.1.2. Aluminium sphere

4.2.1.2.1. Layer part

Figure 4.13 correlates the CoF with the number of cycles for the three tests performed (10 N,15 N and 20 N) using aluminium ball on layered CFRP piece, it can be concluded that the COF presented very different values, which means that CoF is strongly influenced with the variation in applied load. For 10 N applied load, it presents the highest value of CoF, while the other two tests have a similar value of CoF but as the lowest ones. Similarly, to the other CoF's presented before, the running in is present in the first cycles of the test, seen closely on the mini graph, that goes until 5000 cycles. The CoF on the final cycles have a range of values between the 0.17 and the 0.3.

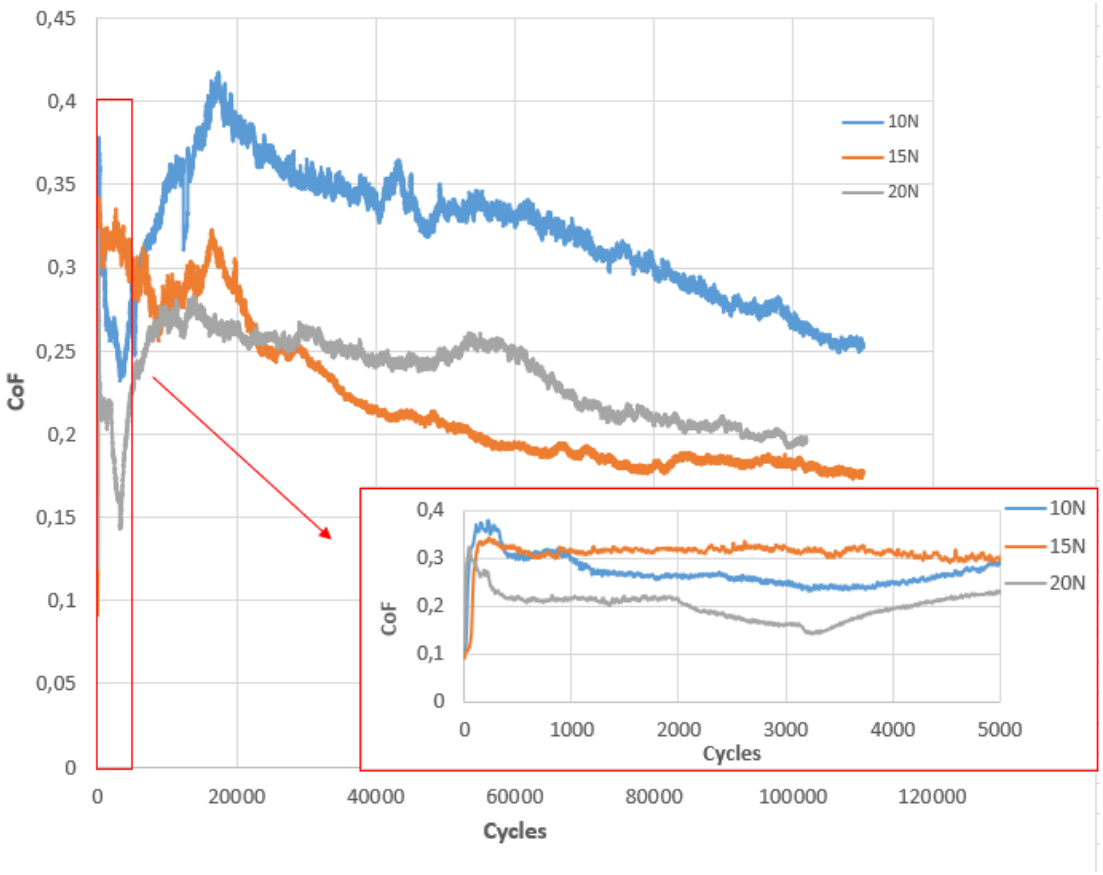

Figure 4.13. Evolution of the CoF with the number of cycles for the CFRP specimen sliding against an aluminium sphere (layer part).

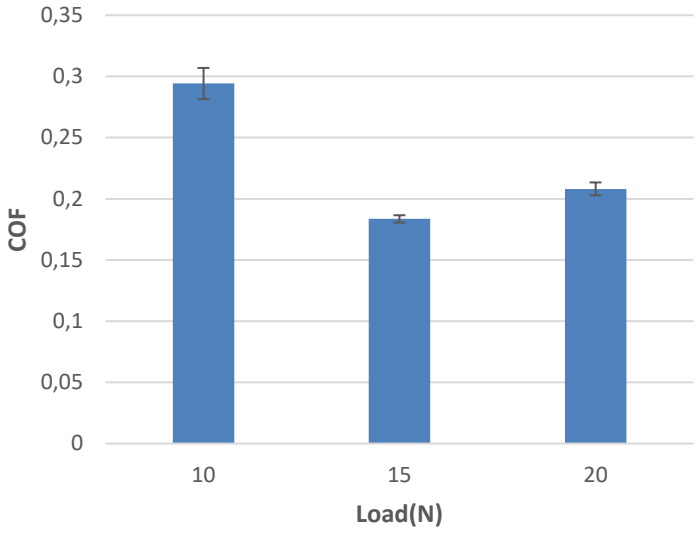

Figure 4.14. Steady state CoF for different applied Loads for the CFRP specimen (layer part) sliding against aluminium spheres.

Similarly, to the other tests, calculation of the average CoF and the standard deviation were made and are presented on Figure 4.14. The Avg CoF was obtained for 25000 cycles (from 70000 until 95000 cycles). The highest CoF belongs to 10 N with a value of 0.29 and the lowest one for 15 N test with a value of 0.18.

4.2.1.2.2. Cross section

After analysing Figure 4.15 that represents the relation between the CoF and the number of cycles of the tests, it is possible to observe, firstly that the data is noisier than the one acquired for the titanium part. Secondly, as happened to the titanium part, it was observed for the first cycles a running in phase followed by a steady state. For these three tests with 10 N, 15 N and 20 N the values pretty much are the same and the CoF doesn't change much between each one of them, having a coefficient of friction in the end rounding the 0.2 and the 0.25. When comparing the layer to the cross section of the aluminium ball, it´s possible to observe that on the cross section, the CoF values are more constant between all the loads, around 0,25, while on the layer part the CoF is very different for each load, having an higher range of CoF values.

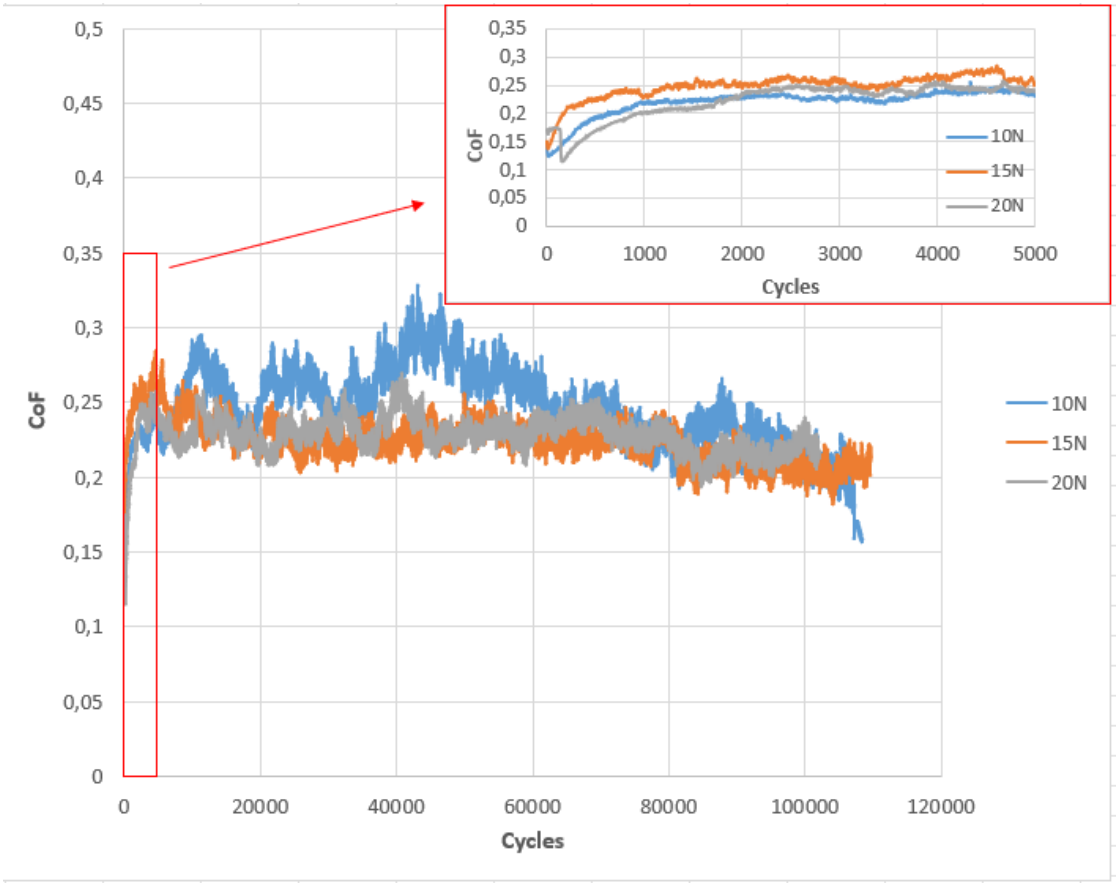

Figure 4.15. Evolution of the CoF with the number of cycles for the CFRP specimen sliding against an aluminium sphere (cross section part).

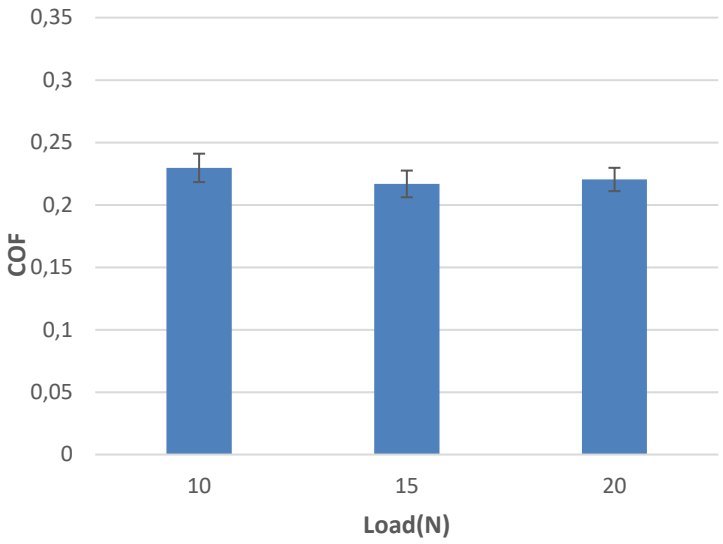

Figure 4.16. Steady state CoF for different applied Loads for the CFRP specimen (cross section part) sliding against aluminium spheres.

The average CoF and standard deviation for each test was acquired and is represented in Figure 4.16. In this case the average CoF and the standard deviation was calculated for 25000 cycles (70000; 95000). By analysing the Figure 4.16, it´s possible to see the constant value of the CoF in all of the tests and that the highest CoF between that 25000 cycles belong to the 10 N test with a value of 0.23, and the lowest CoF for the 15 N test with 0.22.

4.2.2. Wear volume of the CFRP specimens

Prior to conducting profilometry, it was anticipated that the wear volume on the CFRP specimen would be larger when rubbed against a titanium ball, given its higher strength compared to aluminum. Furthermore, when comparing the layer and cross section, it was predicted that the wear volume profile would be higher on the cross section due to its bidirectional nature, which implies lower strength. In order to validate these predictions, graphs are presented below.

4.2.2.1. Titanium ball

4.2.2.1.1. Layer part

Regarding the layer part, Figure 4.17, that compares the depth of the wear track with the transversal length, illustrates that the wear track values remain relatively consistent across the five tests conducted (10 N, 15 N, 20 N, 25 N and 30 N). However, as the load increased, the depth also increased. To determine the average volume of each test, three profiles were integrated. To accomplish this, the profiles were aligned with the xx line and subsequently employed the trapezoid formula to calculate the volume beneath the xx line. Additionally, to determine the K value, which represents the wear coefficient, equation 4.1 was used.

As (Aamir et al. 2019) said, the unidirectional layer has a consistent strength throughout the layer because it consists solely in one orientation of fibers. Due to its consistent strength, it is more resistance to break, which means that is going to have more resistance to wear. As a result, all five tests exhibit very similar volume measurements since they all focus on this layer. Breaking this layer of fiber proves challenging for all tests, making it difficult to transition to the next layer. Consequently, the volume remains relatively consistent, with only a slight increase as the load is incrementally increased.

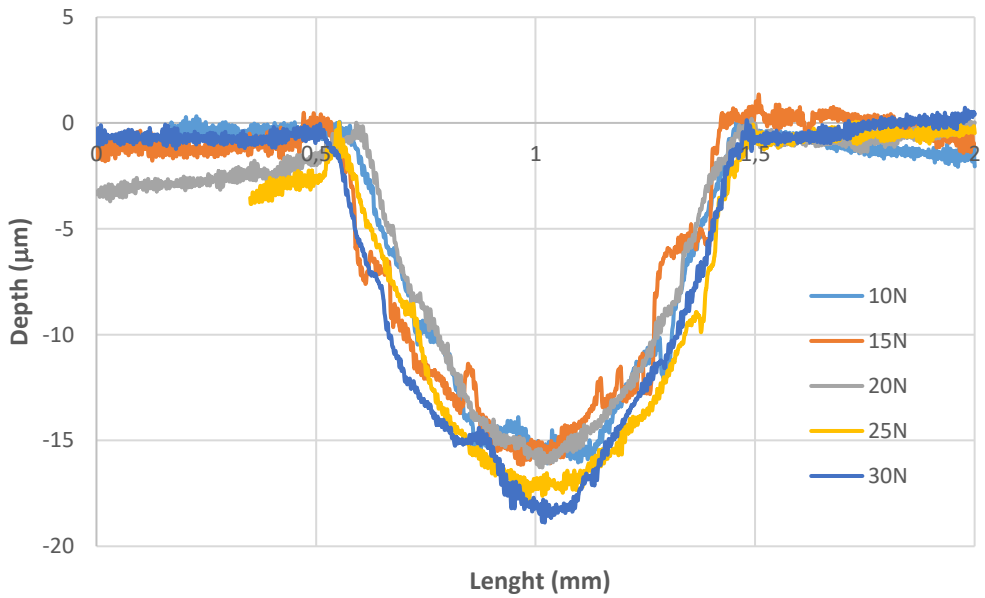

Figure 4.17. 2D profiles from the cross-section wear track of the CFRP specimens (layer part), sliding against a titanium sphere under different applied loads (10, 15, 20, 25 and 30 N).

The formula for calculating the wear rate K is the following:

$$K=\frac{V}{N\times x} \qquad (4.1)$$

K = Wear coefficient (mm^3/N.m)

V = Wear volume (mm^3)

N = Applied load (N)

X = Sliding distance (m)

The average wear volume and average wear rate (K) value were calculated and can be seen in Table 4.1.

Table 4.1. Wear volume and wear rate for CFRP specimens (layer part) sliding against titanium ball.

Applied Load (N)	10	15	20	25	30
K (mm^3/N.m)	2.86E-16	2.19E-16	2.03E-16	1.78E-16	1.48E-16
Volume (mm^3)	1.26E-12	1.92E-12	1.79E-12	1.95E-12	1.95E-12

In Table 4.1, it is evident that both the wear volume and the K value are influenced by the load. As the load increases, we observe a consistent increase in wear volume, with the exception of the 15 N case. Conversely, there is a consistent decrease in the K value. In theory, if the volume increases, the K value should also increase since they are proportionally related in the formula above. However, in this particular scenario, the value of the wear volume is significantly smaller and similar across the tests, whereas the load values are considerably higher. Consequently, the increase in the wear volume is insufficient to compensate for the substantial increase in load, resulting in a decrease in the K value.

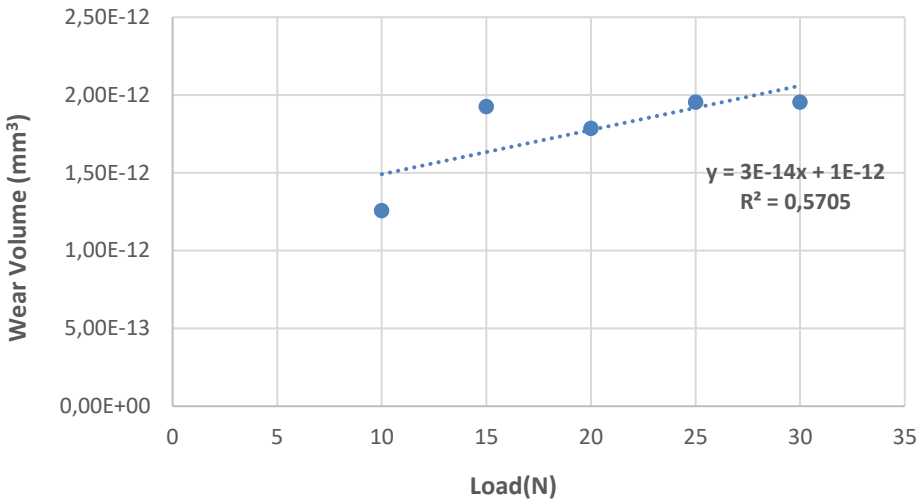

Figure 4.18. Wear volume vs applied Load for the CFRP specimens (layer part) sliding against titanium spheres.

By analyzing Figure 4.18, it is possible to confirm the relationship described in the preceding table, where the values increase proportionally with the load. Furthermore, the graph indicates a trendline, with the data points aligning closely to the expected values on the trendline.

After examining K vs. load presented in Figure 4.19, it becomes evident that the values consistently decrease in proportion to the load. Notably, in this scenario, all the values closely align with the expected trendline, and there are no outlier points, like in the other graph. Thus, every value demonstrates a proportional decrease.

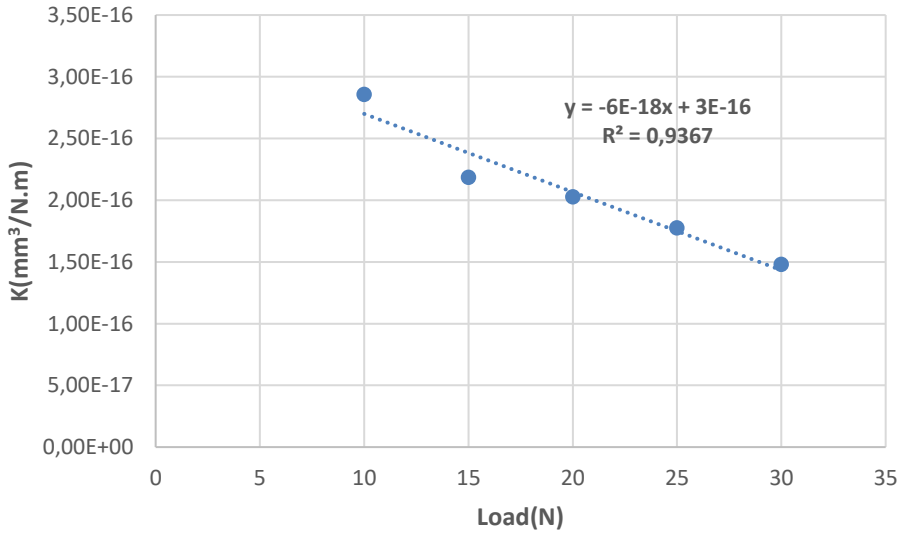

Figure 4.19. Wear rate coefficient vs applied Load for the CFRP specimens (layer part) sliding against titanium spheres.

4.2.2.1.2. Cross section

In reference to the cross section, Figure 4.20 compares the depth with the length of the wear track and there it´s possible to observe that similarly as what happened to the layer part, when the load increases, the volume also increases. We can observe that the volume obtained is very similar during the initial three tests, the ones with low values (10 N, 15 N, 20 N). However, when considering the last two tests with higher loads (25 N and 30 N), we notice their similarity while observing significantly higher volumes compared to the first three tests. For the cross section the 10 N test is the one with lowest wear volume with a value of 6.08E-13 mm^3, and the highest one belongs to the 30 N test with a value of 9.80E-16 mm^3.

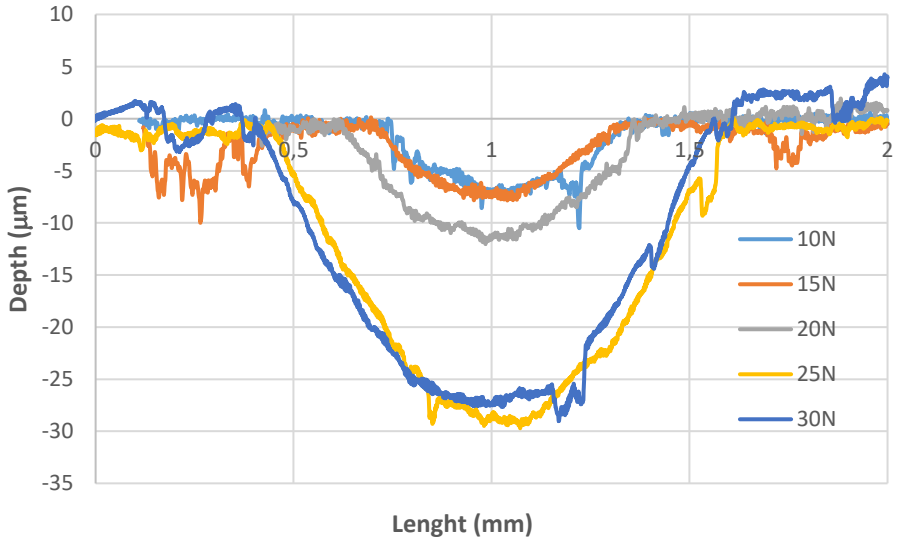

Figure 4.20. 2D profiles from the cross-section wear track of the CFRP specimens (cross section part), sliding against a titanium sphere under different applied loads (10, 15, 20, 25 and 30 N).

Just as in the layer part, the same procedures were followed, including calculating the average wear volume and the K value and are represented in Table 4.2.

Table 4.2. Wear volume and wear rate for CFRP specimens (cross section part) sliding against titanium spheres.

Load (N)	10	15	20	25	30
Volume (mm^3)	6.08E-13	6.48E-13	1.17E-12	7.68E-12	8.62E-12
K (mm^3/N.m)	1.38E-16	9.82E-17	1.33E-16	8.73E-16	9.80E-16

The influence of the load on both wear volume and K values is clearly observed in Table 4.2. As the load increases, there is a noticeable consistent rise in wear volume. Furthermore, it is evident, as previously seen in Figure 4.20, that the two final tests with loads of 25 N and 30 N exhibit significantly different order values compared to the other three tests. However, the relationship between the load and the K value is not as straightforward as for the volume. Unlike volume, an increase in load does not always result in a corresponding increase in the K value, or a decrease.

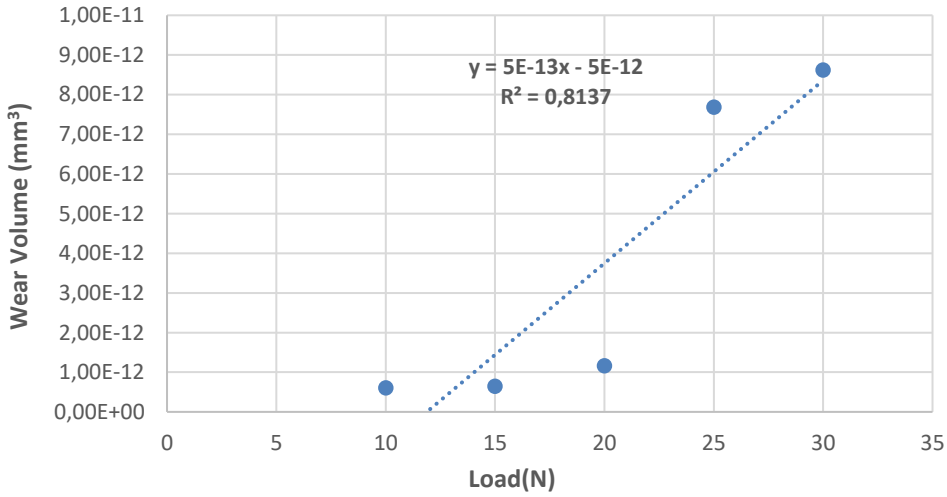

Figure 4.21. Wear volume vs applied Load for the CFRP specimens (cross section part) sliding against titanium spheres.

For Figure 4.21 and Figure 4.22 it´s possible to observe better the influence of the load on the volume and on the K. In the first case, Figure 4.21, we clearly see an increase of the volume was the load increases, and for the last two points a big increase on the volume value as seen on Table 4.2 and on Figure 4.20. The same happened to the K value, Figure 4.22. In a general way the volume and the K followed the trendline values, and increased with the increase of the load, and had big values for the last two loads compared to the first three.

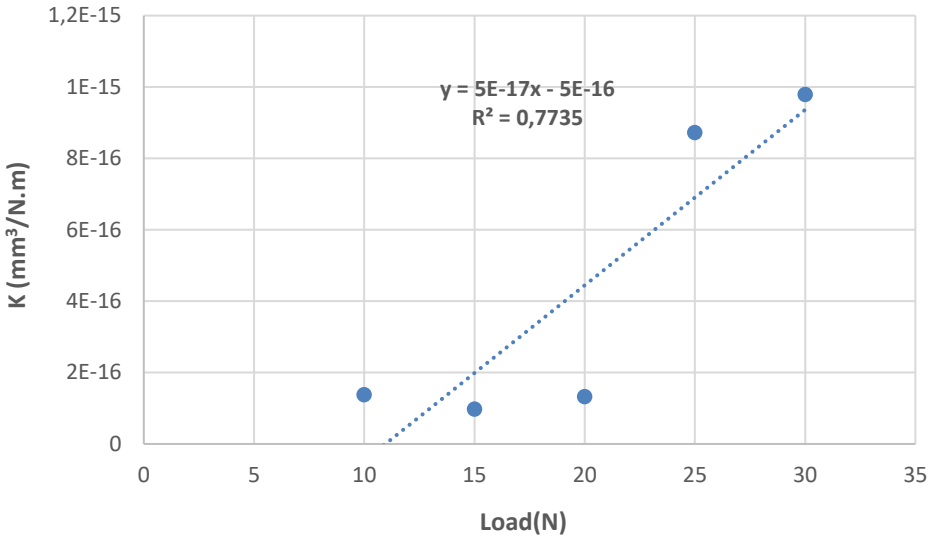

Figure 4.22. Wear rate coefficient vs applied load for the CFRP specimens (cross section part) sliding against titanium spheres.

4.2.2.2. Aluminium spheres

4.2.2.2.1. Layer part

Regarding the layer part, as shown in Figure 4.23, that demonstrates the relationship between the depth and the length of the wear track, it is possible to observe a similar trend to what was observed for the titanium layer part. The values remain relatively consistent, and as the load increases, the volume also increases. However, in this case, the graph displays more pronounced noise compared to the titanium experiments. This variation can be attributed to the lower strength of the aluminum spheres used in the experiments, as compared to the titanium spheres leading to increased transferred aluminium in the CFRP contact. Here, the test with lowest wear volume was with the 10 N with a value of 6.53E-13 mm^3, and the highest wear volume belongs to the 20 N test with a value of 1.15E-12 mm^3. Similarly, with what was observed with the titanium spheres, for the layer part, the wear volume doesn't have a big gap from one load to another.

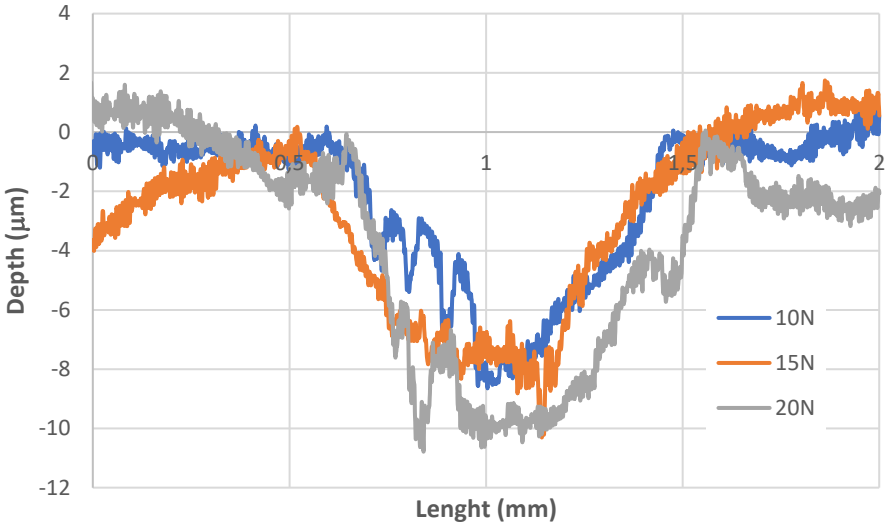

Figure 4.23. 2D profiles from the cross-section wear track of the CFRP specimens (layer part), sliding against an aluminum sphere under different applied loads (10, 15, 20 N).

Table 4.3 show the average wear volume as well the wear rate coefficient, k, that allowed me to create Figure 4.24 and Figure 4.25.

Table 4.3. Wear volume and wear rate coefficient for CFRP specimens (layer part) sliding against aluminum spheres.

Load (N)	10	15	20
Volume (mm^3)	6.53E-13	1.04E-12	1.15E-12
K (mm^3/N.m)	1.48E-16	1.58E-16	1.31E-16

As anticipated for the layer component, similar to the titanium example, the volume increases as the load increases. However, when it comes to the wear rate, K, the results are not as simple. In the initial two tests (10 N and 15 N) the value of the K increased with the increment of the load. However, in the last test (20 N), the value decreased, and it was even lower than the initial measurement for 10 N applied load.

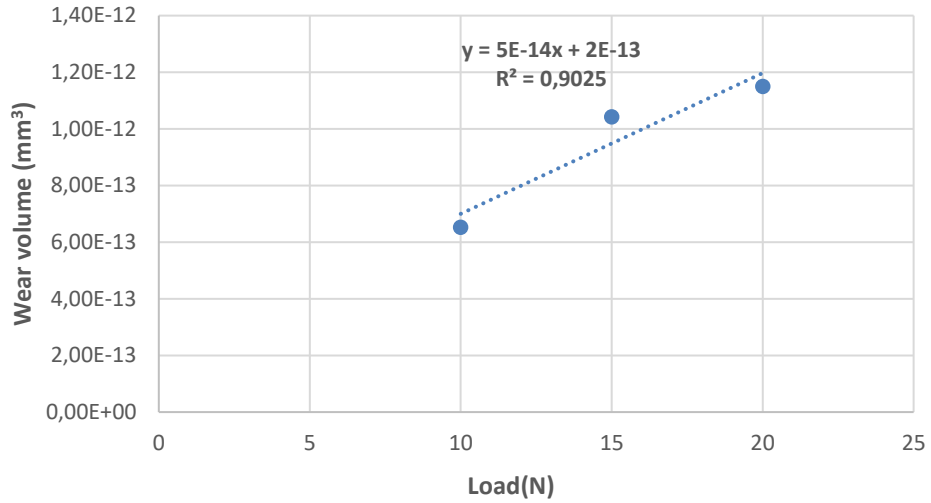

Figure 4.24. Wear volume vs applied Load for the CFRP specimens (layer part) sliding against aluminum spheres

As already seen on Table 4.3, the Figure 4.24 shows that an increase on the load have an increase on the wear volume. But for

Figure **4.25**, the value of the wear rate coefficient, K with the influence of the load, has a fluctuation pattern, because it starts by increasing and then decreases. The trendline expected the values to decrease with the increment of the load, and the only value that doesn't respect that is the 15 N one.

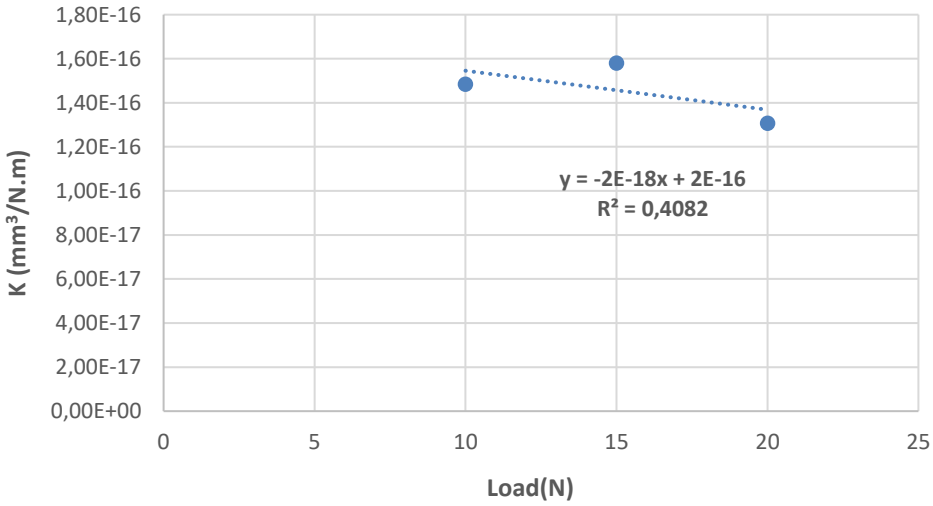

Figure 4.25. Wear rate coefficient vs applied load for the CFRP specimens (layer part) sliding against aluminum spheres.

4.2.2.2.2. Cross section

For the graph that represents the relation between the depth and the length of the wear track, Figure 4.26, it is possible to observe that like what happened to all of the previous graphs, the wear volume increased when the load was increased. In this graph there are 3 different tests representing 10 N, 15 N and 20 N. The one with the lowest volume is the 10 N with a value of 1.86E-12 mm^3, and the one with the highest volume is the 20 N with a value of 8.55E-12 mm^3. Compared to the layer part, here the wear volume is much higher, in the same way that happened on the titanium part. In all of these graphs of the wear volume compared to the length, the one that showed bigger wear volume was this one, referred to the cross section of the CFRP piece that was put against aluminum balls.

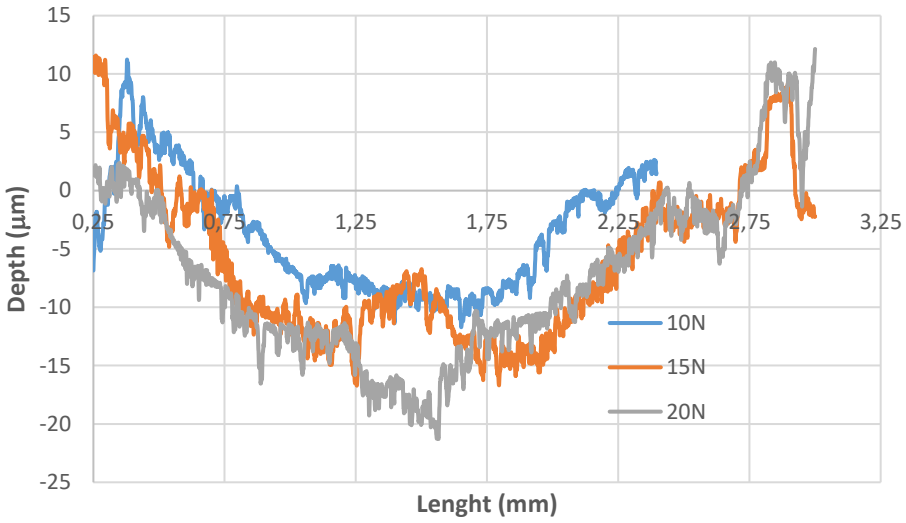

Figure 4.26. 2D profiles from the cross-section wear track of the CFRP specimens (cross section part), sliding against an aluminium sphere under different applied loads (10, 15, 20 N).

The average wear volume between the three profiles for each test was calculated, and the same to the average wear rate coefficient, K. Table 4.4 shows that the wear volume tend to increase with the increasing load, and that the K has a variational comportment to the load, first increasing but later decreasing.

Table 4.4. Wear volume and wear rate coefficient for CFRP specimens (cross section part) sliding against aluminum spheres.

Load (N)	10	15	20
Volume (mm^3)	1.86E-12	6.98E-12	8.55E-12
K (mm^3/N.m)	4.24E-16	1.06E-15	9.71E-16

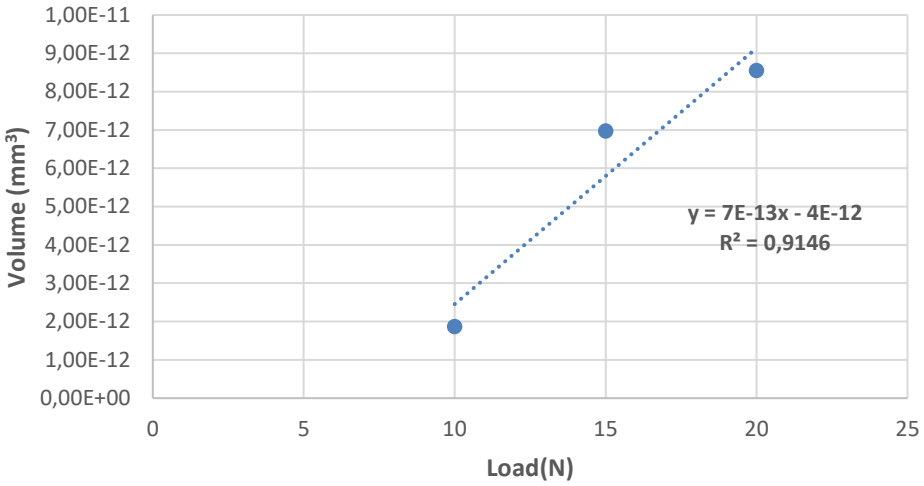

Figure 4.27. Wear volume vs applied Load for the CFRP specimens (cross section part) sliding against aluminum spheres

By analyzing Figure 4.27 and Figure 4.28 the same conclusions can be taken as the ones taken by the observation of Table 4.4 and is that the volume and the K increases every time the load is increased.

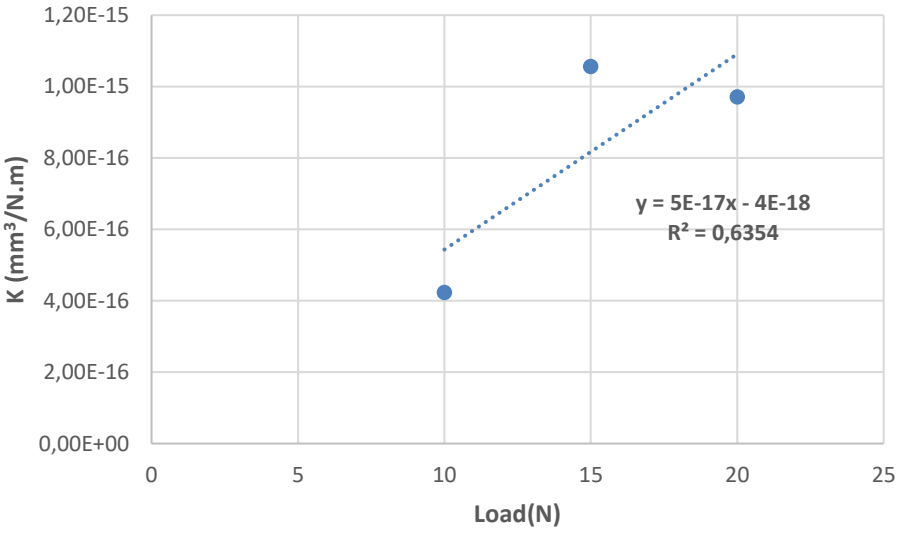

Figure 4.28. Wear rate coefficient vs applied load for the CFRP specimens (cross section part) sliding against aluminum spheres.

4.2.3. Wear mechanism

The provided micrographs on Figure 4.29 clearly show the presence of wear marks on the titanium balls and on the CFRP specimens in all tests, ranging from 10 N to 30 N. All the micrographs shown, presented the same magnification, since the scales are all set to 250 μm for all the titanium spheres, and to 500 μm for all the CFRP specimens. The left side of the micrographs show the results of the five tests conducted on the layer part of the specimen, while the right side displays the outcomes for the cross-section tests. Upon careful analysis of the micrographs, we can draw the same conclusion as the one gotten from the wear volume graphs, which indicates that the wear value increases proportionally with the applied load. This observation is consistent with the images, as the wear marks become progressively larger every time the load is increased. However, it is noteworthy that the 15 N test on the surface layer deviates from this trend, as its wear marks appears significantly larger compared to the others. And on the two last tests of the cross section (right side), we have the highest wear volume when compared to all the tests, and we can see that between those two tests and the first three for the same part, we have a huge gap on wear volume, something already seen on Figure 4.20. Regarding the fiber orientation the Figure 4.29 shows that the wear marks for the layer part is very constant through all the tests meanwhile on the cross section differences on the wear marks are observed. It is possible to see that each micrograph of the titanium sphere, having in consideration the load and the part where the test was conducted, corresponds to the micrograph taken on the CFRP specimen. On the micrographs of the CFRP specimen for the cross section, with closer attention is possible to see the bidirectional orientation of the fibers and that in some areas the wear is bigger than in the others, this is due to the bidirectionality like (Aamir et al. 2019) said. On the layer part, which means unidirectionality of fibres, it is possible to observe that just one direction of the fibres is in contact. But, in a few areas and normally on the highest loads, some breaking of the first layer and appearance of the second one is possible to see.

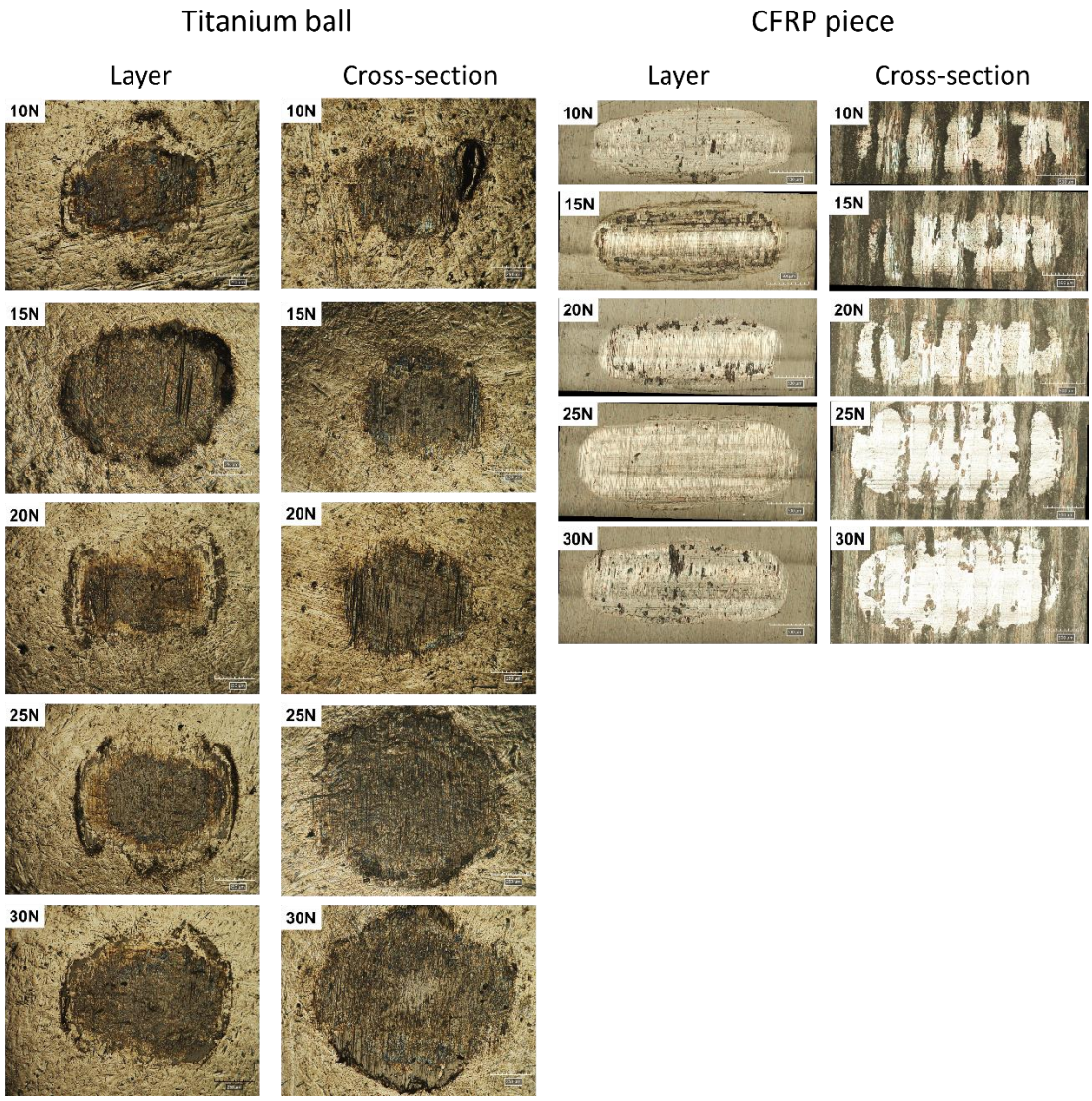

Figure 4.29. Optical micrographs from the body (CFRP specimen) and counter bodies (spheres) on the titanium ball tests.

The following micrographs, Figure 4.30, shows the wear marks on the aluminium spheres and on the CFRP specimen in all of the tests, from 10 N to 20 N, being the left side for the three tests from the layer part and the right side the three tests for the cross section. The magnification from one side to the other is different, being for the left side 500 μm the scale and for the left side the scale is 1000 μm. This difference on the scale happened because of the wear mark from the cross section being bigger, which means it was needed to reduce

the magnification in order to see all the mark. By analyzing the micrographs, it´s possible to observe that, like the same way that happened to titanium with higher loads we have bigger wear marks and deeper ones, something that we already understood from the wear volume graphs. Comparisons between the layer part and the cross section are clear, because the scale change tell us that one mark is bigger than other, and in this case the cross section marks have a higher scale which means that on the cross section we have a higher wear marks when compared to the layer. By comparing the wear marks on the titanium and aluminium spheres, bigger marks on the aluminium spheres were observed due to the wear. This happened, because the scale on the titanium photos is smaller (250μm) than the one on the aluminium photos (500 μm or 1000 μm). From the different parts on the titanium spheres significant differences are not seen, because they all have the same values, while on the aluminium spheres a big difference is seen between the part where the tests are done, due to the change of magnification, which means bigger wear marks.

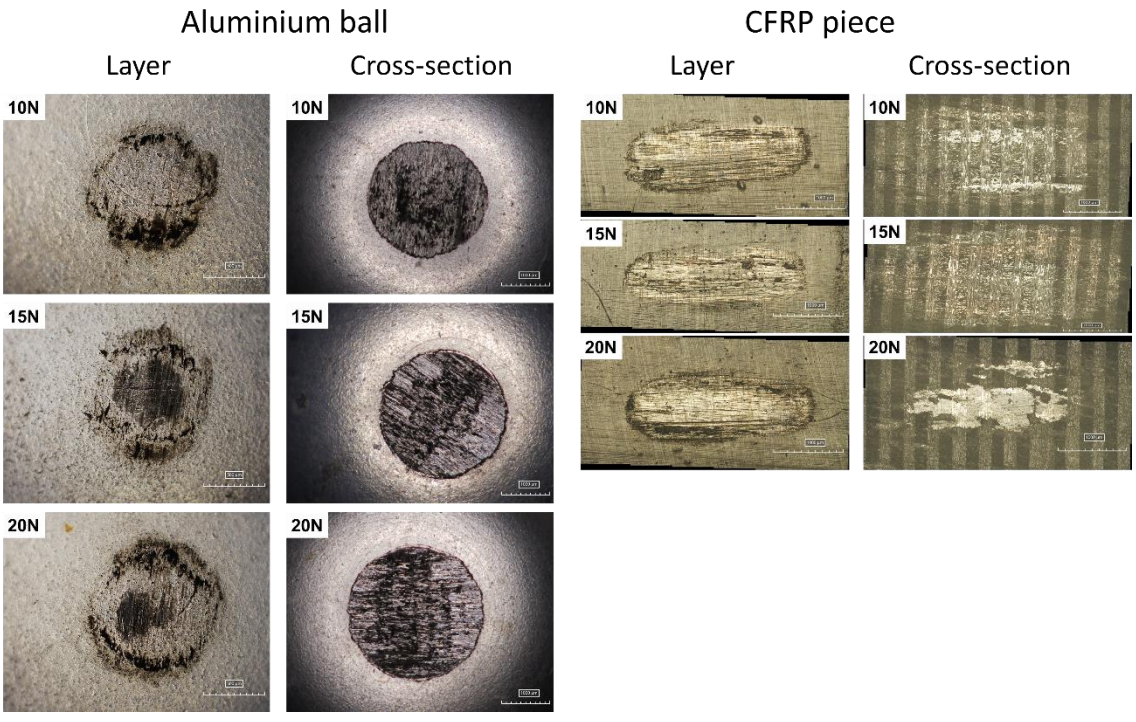

Figure 4.30. Optical micrographs from the body (CFRP specimen) and counter bodies (spheres) on the aluminum ball tests.

5. CONCLUSIONS

The main objective of the present research work, was to understand better the mechanical and tribological behavior of the carbon fiber reinforced polymer when on a situation of supposed drilling. After all the tribological tests, characterization, demonstration of the results and respective discussion, the following conclusions were possible to obtain:

- The CoF is dependent on the load, on the fiber orientation and on the material in use (counter body).
- For the first part of the work the CoF of the titanium is higher when compared to the CoF of the CFRP, and the CoF tends to get higher on the tests with higher loads, having an increase of the COF with an increase on the load.
- On the hybrid ring there are fluctuations on the CoF due to the change of material on the ring, and it´s possible to see the peaks of CoF in the beginning, being the higher one for titanium and the lowest one for CFRP. With time passing by we see a more similarity CoF, with less fluctuation, due to the share of material in all of the ring.
- In the second part of the tests the CoF has a higher value when on the layer part of the CFRP specimen compared to the one felt on the cross section, either for titanium or for aluminium.
- When in comparison the influence of the material (titanium or aluminium), the CoF felt on the titanium is lower when compared to the aluminium.
- The wear volume in all of the tests follows the same principle, that with an increase of the load, the wear volume increases. In the first part we have more wear volume for the titanium compared to the CFRP, and in the same way on the hybrid ring the wear volume is bigger in titanium.
- For the second part, when regarding the material, the wear volume is bigger for the aluminium tests, and regarding the location of the test, the wear volume is bigger for the cross section.

5.1. Suggestion for future work

In scientific research we can never say that all the work was done, because there is always something that we could have done more or even better, such as, repetition of the tests for better data acquirement, repetition of some characterization, or even study the same tests but for different conditions or different materials.

In my work the main goal was reached that was to characterize the mechanical and tribological behavior of the CFRP, but some other things could have been done:

- Study the same tests done in this work but this time doing it with lubrication, instead of dry conditions testing, to see the effect of the lubrication on the CoF and on the wear mark.
- Conducted some other tests to increase loads and sliding times to see if the CoF will remain the same independently of the sliding time and loads.
- Change the counter bodies of the balls, for example using of a ball of aluminium but this time not anodized.

REFERENCES

Aamir, Muhammad, Majid Tolouei-Rad, Khaled Giasin, and Ataollah Nosrati. 2019. "Recent Advances in Drilling of Carbon Fiber–Reinforced Polymers for Aerospace Applications: A Review." *International Journal of Advanced Manufacturing Technology* 105(5–6):2289–2308. doi: 10.1007/s00170-019-04348-z.

Birleanu, Corina, Marius Pustan, Grigore Pop, Mircea Cioaza, Florin Popa, Lucian Lazarescu, and Glad Contiu. 2022. "Experimental Investigation of the Tribological Behaviors of Carbon Fiber Reinforced Polymer Composites under Boundary Lubrication." *Polymers* 14(18). doi: 10.3390/polym14183716.

Dong, H. 2010. "Tribological Properties of Titanium-Based Alloys." Pp. 58–80 in *Surface Engineering of Light Alloys: Aluminium, Magnesium and Titanium Alloys*. Elsevier Inc.

Hu, Junshan, Kaifu Zhang, Qingda Yang, Hui Cheng, Shunuan Liu, and Yu Yang. 2017. "Fretting Behaviors of Interface between CFRP and Coated Titanium Alloy in Composite Interference-Fit Joints under Service Condition." *Materials and Design* 134:91–102. doi: 10.1016/j.matdes.2017.08.018.

Khan, Sharjeel Ahmed, Nazanin Emami, and Amilcar Ramalho. 2023. "Custom-Tailored Cross-Cylinder Tribotest to Emulate Wear Mechanism in Drilling of CFRP-Ti Stacks." *Tribology International* 186. doi: 10.1016/j.triboint.2023.108589.

Li, Jian, Kaifu Zhang, Ping Liu, and Yuan Li. 2018. "Tribological Behavior and Microstructure of Carbon Fiber–Reinforced Polymer against Ti6Al4V Alloy in Fretting Contact." *Tribology Transactions* 61(2):256–68. doi: 10.1080/10402004.2017.1313471.

Liang, Xiong, and Dan Wu. 2019. "Tribological Properties of Carbon-Fibre-Reinforced Plastic against Tungsten Carbide under Dry Condition." *Tribology International* 134:118–28. doi: 10.1016/j.triboint.2019.01.043.

Nguyen, Dinh, Mohammad Sayem Bin Abdullah, Ryan Khawarizmi, Dave Kim, and Patrick Kwon. 2020. "The Effect of Fiber Orientation on Tool Wear in Edge-Trimming of Carbon Fiber Reinforced Plastics (CFRP) Laminates." *Wear* 450–451. doi: 10.1016/j.wear.2020.203213.

Shyha, Islam, Sein Leung Soo, David K. Aspinwall, Sam Bradley, Stuart Dawson, and Cornelius J. Pretorius. 2010. "Drilling of Titanium/CFRP/Aluminium Stacks." Pp. 624–33 in *Key Engineering Materials*. Vol. 447 448. Trans Tech Publications Ltd.

Stachowiak, Gwidon W., and Andrew W. Batchelor. n.d. *E N G I N E E R I N G T R I B O L O G Y*.

Suo, Haoyuan, Zhaohui Wei, Kaifu Zhang, Kelin Deng, Hui Cheng, Bin Luo, Hailin Li, Linxuan Wang, and Biao Liang. 2022. "Interfacial Wear Damage of CFRP/Ti-Alloy Single-Lap Bolted Joint after Long-Term Seawater Aging." *Engineering Failure Analysis* 139. doi: 10.1016/j.engfailanal.2022.106464.

Valentin Popov. n.d. *Contact Mechanics and Friction: Physical Principles and Applications*.

Wang, Xin, Parick Y. Kwon, Caleb Sturtevant, Dave Dae Wook Kim, and Jeff Lantrip. 2014. "Comparative Tool Wear Study Based on Drilling Experiments on CFRp/Ti Stack and Its Individual Layers." *Wear* 317(1–2):265–76. doi: 10.1016/j.wear.2014.05.007.